

REPUBLIC OF TURKEY
YUZUNCU YIL UNIVERSITY
INSTITUTE OF HEALTH SCIENCE

**A STEREOLOGICAL STUDY ON THE MOTOR NEURON NUMBER IN
SPINAL CORD SEGMENT T11 IN DIFFERENT DOSES OF
STREPTOZOTOCIN ADMINISTERED RATS**

Omed Omer RAHIM
DEPARTMENT OF MEDICAL HISTOLOGY AND EMBRYOLOGY
(MEDICAL PROGRAM)
MASTER THESIS

SUPERVISOR

Prof. Dr. Murat Çetin RAĞBETLİ

VAN – 2017

REPUBLIC OF TURKEY
YUZUNCU YIL UNIVERSITY
INSTITUTE OF HEALTH SCIENCE

**A STEREOLOGICAL STUDY ON THE MOTOR NEURON NUMBER IN
SPINAL CORD SEGMENT T11 IN DIFFERENT DOSES OF
STREPTOZOTOCIN ADMINISTERED RATS**

Omed Omer RAHIM
DEPARTMENT OF MEDICAL HISTOLOGY AND EMBRYOLOGY
(MEDICAL PROGRAM)
MASTER THESIS

SUPERVISOR

Prof. Dr. Murat Çetin RAĞBETLİ

VAN – 2017

This master thesis study was supported by research fund (BAP) of Yuzuncu Yil
University Project No: TYL-2016-5507

REPUBLIC OF TURKEY
YUZUNCU YIL UNIVERSITY
INSTITUTE OF HEALTH SCIENCE

**A STEREOLOGICAL STUDY ON THE MOTOR NEURON NUMBER IN
SPINAL CORD SEGMENT T11 IN DIFFERENT DOSES OF
STREPTOZOTOCIN ADMINISTERED RATS**

Omed Omer RAHIM
DEPARTMENT OF MEDICAL HISTOLOGY AND EMBRYOLOGY
(MEDICAL PROGRAM)
MASTER THESIS

Prof. Dr. Murat Çetin RAĞBETLİ
Head of Jury

Assoc. Prof. Dr. Levent TMKAYA
Member

Asst. Prof. Dr. NeŐe LİMEN
Member

THESIS ADMISSION DATE

8.5. 2017

Acknowledgments

Praise to Allah, Lord of the World's First and above all, the almighty for providing me with this opportunity and granting me the capability to proceed successfully. This thesis appears in its current form due to the assistance and guidance of several people. I would, therefore, like to offer my sincere thanks to all of them:

Prof. Dr. Murat Çetin RAĞBETLİ, my teacher, and my Supervisor, esteemed promoter, my cordial thanks for accepted me as a MSc. the student in your department, your warm encouragement, thoughtful guidance, and correction of the thesis. Besides my advisor, I would like to thank the rest of my thesis committee for their encouragement, insightful comments, and questions. I would like to thank everyone from Yrd. Doç Dr. Okan ARHAN, Doç Dr. Halil ÖZKOL, Yrd. Doç Dr. Neşe ÇÖLÇİMEN for helping me during check my thesis. My sincere thanks also go to Veysel Akyol for offering me for his help during my study and help me during my thesis's work. I thank my fellow labmates in histology and embryology department: Fikrat Altındağ, Seda Keskin, Tahir İgit, Suleyman Taşkın and all staff in Histology and Embryology Department for help and all the fun we have had in the last two years. And I thanks to the BAPB of Yuzuncu Yıl University for their supporting.

Last but not the least, I would like to thank my family, my Mother, my brother in the same time my friend, my lovely wife and my children, for all him supporting me throughout my life.

Dedication to the spirit of my father

For this day I wished the first one that I see after finish from my study is my father. You made me live this world with great happiness. Thanks for everything.

CONTENTS

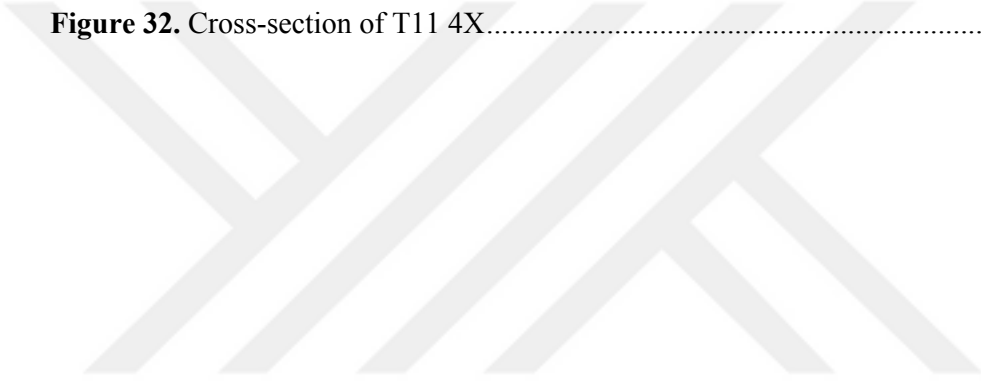
CONTENTS.....	IV
FIGURES.....	VI
TABLES	XIII
ABBREVIATIONS	IX
1. INTRODUCTION	1
2. GENERAL INFORMATION.....	3
2.1. Diabetes Mellitus	3
2.1.1 Diabetes history.....	3
2.1.1.1 History of diabetes in antiquated Egypt	4
2.1.1.2 History of diabetes in antiquated India and China	4
2.1.1.2 History of diabetes in islamic world.....	5
2.1.2 Diabetes types	6
2.1.2.1 Diabetes type I insulin-dependent diabetes mellitus (IDDM).....	6
2.1.2.2 Diabetes type II non-insulin-dependent diabetes mellitus (NIDDM)	6
2.1.2.3 Gestational diabetes mellitus (GDM).....	7
2.1.3 Experimental diabetes	7
2.2. Spinal Cord	8
2.2.1 Embryology of spinal cord.....	10
2.2.2 Anatomy of spinal cord.....	13
2.2.3 Histology of spinal cord	14
2.2.4. Physiology of spinal cord.....	16
2.3. T11 Segment.....	17
2.4. Motor Neuron (Motoneurons)	17
2.5. Streptozotocins.....	18

2.6. Stereological Methods	19
2.6.1 Disector	25
2.6.2 Physical disector:	26
2.6.3 Counting frame.....	29
2.6.4 Measuring cross-section thickness	30
2.6.5 Fractionation	31
2.6.6 Physical fractionation:.....	32
2.6.7 Pointed area measurement scale.....	34
2.6.8 Application of disector cavalieri	35
3. MATERIALS AND METHODS.....	38
3.1. Materials.....	38
3.2. Application of Experiment.....	38
3.3. Histological Staining Process.....	46
3.4. Chemical Substances Used	47
3.5. Devices.....	47
4. RESULTS	49
4.1. Statistical Description.....	49
5. DISCUSSION AND CONCLUSION	59
SUMMARY	64
ÖZET	65
REFERENCES	66
CURRICULUM VITAE.....	77
ATTACHMENTS.....	78
1. Plagiarism Result	78

FIGURES

Figure 1. The Ebers papyrus	4
Figure 2. Lateral and Medial longitudinal transaction	9
Figure 3. Neural plate and neural tube formation	11
Figure 4. Location of spinal cord and Positional Changes	13
Figure 5. The gross anatomy of the spinal cord	14
Figure 6. Laminar organization	15
Figure 7. Reflex arc	17
Figure 8. Summary diagrams of the locations of some identified neuron systems	18
Figure 9. Chemical structural formula of a streptozotocin	19
Figure 10. Size reduction in specimens	20
Figure 11. Effect of particle size and orientation on sampling chance	21
Figure 12. The relationship between the direction of equally spaced cross-sections	22
Figure 13. Schematic representation of the physical fragmentation method	23
Figure 14. Schematic representation of physical discrete application	27
Figure 15. Neutral census framework	30
Figure 16. Example of a dotted area measurement ruler	35
Figure 17. Cages in which the animals are housed	38
Figure 18. Left intraperitoneally injection	39
Figure 19. A-Tacked blood from tail , b-The used blood glucometer	40
Figure 20. Perfused process until bleaching.	41
Figure 21. A-removed the Thoracic diaphragm, b- Vertebratomy	42
Figure 22. The T11 spinal cord segment 2mm.	43
Figure 23. T11 segment of Spinal cord sectioning.	44
Figure 24. Cross section of T11 segment of Spinal cord sectioning 4X.....	54

Figure 25. Cross section of T11 segment of Spinal cord sectioning 10X.....	54
Figure 26. Motor neuron cell 40X	55
Figure 27. Motor neuron cell 100X	55
Figure 28. Motor neuron cell 100X	56
Figure 29. Motor neuron cell 100X	56
Figure 30. Cross-section diagram of T11 4X.....	57
Figure 31. Cross-section of T11 4X.....	57
Figure 32. Cross-section of T11 4X.....	58



TABLES

Table 1. Descriptive statistics and comparison results.....	50
Table 2. Net weight and percentage Net weight and percentage	51
Table 3. Weight change in groups.....	52
Table 4. Blood glucose levels change Blood glucose levels change	50
Table 5. Total motor neuron number and area values.....	53



ABBREVIATIONS

ATP-PCr	: Adenosine Triphosphate-Phosphocreatine
°C	: Degrees Celsius
CNS	: Central nervous system
CSF	: Cerebrospinal Fluid
DM	: Diabetes mellitus
G45	: Rats Group that injected by 45g/kg of STZ
G65	: Rats Group that injected by 65g/kg of STZ
GDM	: Gestational Diabetes Mellitus
IDDM	: Insulin-Dependent Diabetes Mellitus
NAD	: Nicotinamide Adenine Dinucleotide
NIDDM	: Non-Insulin-Dependent Diabetes Mellitus
OsO ₄	: Osmium tetroxide
Pc	: Post-Conception or post-origination
PNS	: Peripheral Nervous System
SPSS	: Statistical Package for the Social Sciences
SRS	: Systematic Random Sampling
STZ	: Streptozotocin
T11	: 11 th Thoracic segment of spinal cord or 11 th thoracic vertebrae
T1D	: Type one Diabetes
T2D	: Type two Diabetes
TEM	: Transmission electron microscopy
WHO	: World Health Organization
β-cell	: Beta cell
μm	: Micrometer

1. INTRODUCTION

The sources of energy and food to human are carbohydrate, fat, protein, ATP-Pcr and micronutrients. The physiological disorder or a disease that causes blocking these resources to reach the cells of the body or deficiency of these resources are one of the cause that producing diseases in human. Sugar is the popularized name for sweet, short-chain, solvent starches (carbohydrates), a large portion of which are utilized as a part of nourishment. The basic atom of sugar having the important role in the building new cells and obtaining energy, sugar is one of the sources of energy, the human taking the sugar orally as food for performing his daily activity in normal condition (Devlin, 1997; Vasudevan et al., 2013).

To demonstrate any morphometric change in the organism's body due to diseases, we need a scientific method like stereological science and information to know how these diseases occur and on any organ, tissues and a cell that influence, to proof that the change occurs or not. So we need the scientific method like histology science. Precise technique, good preparation, achievement of tissues and cells are needed to confirmation of the changes. Diabetes mellitus (DM) general names that indicated to diabetes. DM is a collection and series of metabolic illnesses in which there are high glucose levels present in the blood for long period. Related to different metabolic issue (Seino et al., 2010).

DM is the disease of antiquity, It's a standout amongst an essential medical issue around the world, indicating high lists of commonness and mortality (Alarcon-Aguilar et al., 2000). Diabetes mellitus can be characterized as a gathering of metabolic infections portrayed by incessant hyperglycemia, coming about because of deformities in insulin emission, insulin activity, or both, offering to ascend to weakened capacity in the sugar, lipid and protein digestion system (Kuzuya et al., 2002) diabetic mellitus one of the diseases that occur by physiological disorder or by outside body effects such as drug or eating poison thing. Diabetes has the ancient history in the world of humans (Beauquis et al., 2008).

The incessant confusion of the disease induces trouble in the visional system, kidney, heart, and blood vessels (Beauquis et al, 2008; Oliveira et al., 2013; Sato et

al., 2014). As well, the nerves system is also damaged give rise to drawback at the CNS (central nervous system) and PNC (peripheral nervous system) layer (Zochodne et al., 2008). Diabetic neuropathy is the most surely implied neuropathy in modern countries, and it is connected with a broad assortment of clinical appearances. Diabetes mellitus is the most well-known reason for neuropathy worldwide (Said, 2007). The enlistment of trial diabetes in the rat utilizing chemicals which specifically pulverize pancreatic β cells are extremely helpful and easy to utilize (Szkudelski, 2001). Alloxan and streptozotocin (STZ) are broadly used to instigate exploratory diabetes in creatures (Szkudelski, 2001). STZ is less toxic than alloxan and mortality rate of animals is found less by STZ than alloxan for that, the STZ is best producing diabetes in Rat and in another experimental animal (Hoftiezer and Carpenter, 1973).

The stereological method that means we make comments on the three-dimensional properties of the structures, based on the data obtained from Two-dimensional sections of three-dimensional samples (biological structures, etc.) it is a fully unprejudiced and appropriate technique for ascertaining the volume, numerical layer of format (Gundersen et al., 1988).

The aim of this study was to investigate the different dose applied to adult rats at different doses using stereological methods because we did not find a stereological study that showed the effects of diabetes on the total number of motor neurons in the rat medulla spinalis T11 segment.

2. GENERAL INFORMATION

2.1. Diabetes Mellitus

Diabetes mellitus (DM) is the most widely recognized metabolic troubles in human being including a gathering of related ailments portrayed by hyperglycemia thus of deficient insulin discharge, insulin resistance, or both. The long haul intricacies of the ailment influence the visual framework, kidneys, heart, and veins (Gispén and Biessels, 2000; Beauquis et al., 2008; Oliveira et al., 2013; Sato et al., 2014). Additionally, the Nervous System is likewise influenced prompting to difficulties at the CNS (Central Nervous System) and PNS (Peripheral Nervous System) levels. Vitality, both Insulin and its receptor are available in the CNS (Gispén and Biessels, 2000; Zochodne et al., 2008; Benitez, 2015)

Causes of Diabetes, it's recognized as a heterogeneous condition (Alberti, 1998) because the reasons are different, for example, lacking creation of insulin (either completely or about the body's needs), generation of faulty insulin, The failure of the cells to utilize insulin legitimately and productively prompts hyperglycemia are some of those reasons (Malgaonkar et al., 2016). Induction of diabetes with streptozotocin decreases nicotinamide adenine dinucleotide (NAD) in pancreas islet beta cells and causes histopathological effects in beta cells which probably intermediates induction of diabetes (Akbarzadeh et al., 2007).

Induction of diabetes with streptozotocin decreases nicotinamide-adenine dinucleotide (NAD) in pancreas islet beta cells and causes histopathological effects in beta cells which probably intermediates induction of diabetes (Akbarzadeh et al., 2007).

2.1.1 Diabetes history

Before named the diabetes mellitus it recognized by his symptoms. It's the one of most established infection known by the human.

2.1.1.1 History of diabetes in antiquated Egypt

A restorative condition creating unnecessary thirst, consistent pee and extreme weight reduction has intrigued medicinal creators for more than three centuries. Sadly, until the early piece of 201h century, the forecast for a patient with this condition was no superior to anything it was more than 3500 years prior in antiquated Egypt (Figure 1) (Ahmed, 2002).

Since the antiquated doctors portrayed only instances of what is today known as type I diabetes mellitus, the result was constantly deadly. Ebers papyrus, which was composed around 1550 BC, exhumed in 1862 AD from an old grave in Thebes of Egypt, and distributed by Egyptologist Georg Ebers in 1874, portrays, among different illnesses and their cures, a state of "excessively incredible exhausting of the urine" perhaps, the reference to diabetes mellitus (Ahmed, 2002; Poretsky, 2004).



Figure 1. The Ebers papyrus. Courtesy of the Wellcome Library, London(Richard et al., 2010)

2.1.1.2 History of diabetes in antiquated India and China

In the fifth century AD, Sushruta and Charaka two Indian physicians, they watched that the pee of individuals with diabetes pulled in ants and flies. They named the condition "madhumeha" or "honey urine". Indian doctors additionally

noticed that patients with "madhumeha" experienced extraordinary thirst and foul breath (probably, from ketosis) despite the fact that the polyuria related with diabetes was very much perceived, antiquated clinicians couldn't recognize the polyuria because of what we now call diabetes mellitus from polyuria because of different conditions. In seventh century AD in China, Li Hsuan noticed that the patients with diabetes were inclined to bubbles and lung diseases. He recommended evasion of sex and wine as treatment for diabetes (Medvei and Cornelius, 1982).

2.1.1.2 History of diabetes in islamic world

Avicenna or Ibn-Sina (980–1037 AD) doctor to caliphs of Baghdad ordered through restorative content (Canon Avicennae), which incorporated a point by point portrayal of diabetes. Its clinical components, for example, sweet pee and expanded hunger, and entanglements, for example, diabetic gangrene and sexual brokenness, were depicted by avicenna in detail (Hosseinzadeh and Nassiri-asl, 2013).

In 1936, Harold Himsworth suggested that there were no less than two clinical sorts of diabetes, insulin delicate and insulin-obtuse. He proposed that insulin-touchy diabetics were insulin lacking and required exogenous insulin to survive, while the other gathering did not require insulin. This perception depended on clinical proof, as around then no examines were accessible for the estimation of insulin (Himsworth HP, 1939). The Australian researcher, Joseph Bornstein, who built up the main bioassay for insulin and was in the end granted a Nobel Prize, at first increased little acknowledgment for his work until he went to work in London with Robin Lawrence (Bornstein, 1951). Taking after the improvement of the bioassay for insulin and its estimation in people with diabetes, it turned out to be progressively obvious that there were no less than two noteworthy unmistakable types of diabetes. With the assistance of the measure, these were presently not just distinct on the premise of age at diabetes onset, additionally by the levels of endogenous insulin. The distinction image at onset prompted the utilization of the terms 'adolescent onset' and 'development onset' diabetes which was thought to be to a great extent steady with their watched treatment contrasts portrayed as insulin-ward diabetes mellitus (IDDM) and non-insulin subordinate diabetes mellitus (NIDDM) (Courten, 2002).

2.1.2 Diabetes types

According to the reason for increasing the level of glucose in the blood than the normal range the type of diabetic differentiated (Malgaonkar et al., 2016).

2.1.2.1 Diabetes type I insulin-dependent diabetes mellitus (IDDM)

From the name, the pancreas could not produce insulin, for that, the patient rely on upon the insulin that taking. Nobody knows for beyond any doubt why individuals get type one diabetes (T1D). A few people are conceived with genes that make them more inclined to get it (Risch, 1987). In any case, numerous other individuals with those same genes don't get diabetes. Something else inside or outside the body triggers the illness. Specialists don't comprehend what that something is yet. Be that as it may, they are attempting to discover (Xu et al 2002).

The vast majority with T1D have elevated amounts of autoantibodies in their blood before they are initially analyzed. Antibodies are proteins your body makes to demolish microorganisms or infections. Autoantibodies assault your body's own tissues (Ziegler et al., 1990). In individuals with type 1 diabetes, autoantibodies may assault the cells in the pancreas that make insulin (Ko et al., 1998).

2.1.2.2 Diabetes type II non-insulin-dependent diabetes mellitus (NIDDM)

In type two diabetes (T2D), your body does not make enough Insulin, or experiences difficulty utilizing the insulin or both (Martin, 1992). A man with type 2 diabetes may require insulin to control blood glucose levels however does not rely on upon it to live. In the event that there is insufficient Insulin or if it's not working right, your cells can't utilize the glucose in your blood to make vitality (Hales and Barker, 1992). Rather, glucose remains in the blood. This can prompt to high blood glucose levels. After some time, high blood glucose levels may hurt your eyes, kidneys, nerves, heart, and veins (Bailes and Bakewell, 2002).

A great many people who get type 2 diabetes are more than 40 years of age. Be that as it may, type 2 diabetes frequently happens in more youthful individuals even youngsters (American Diabetes Association, 2000). In any case, Type II

diabetes frequently happens in more youthful individuals even youngsters. Regularly, the indications of illness might be so mellow or grow so bit by bit that they go unrecognized by the individual with the turmoil (Bardsley, 2004).

Consequently, it is critical that individuals who are at hazard for Type 2 diabetes have blood glucose testing every 3 years to see whether they have diabetes. A portion of the hazard components for type 2 diabetes include: having a parent, sibling, or child with Type II diabetes (Horikawa et al., 2000) or being overweight (Reaven, 1988; Kahn et al., 2006).

2.1.2.3 Gestational diabetes mellitus (GDM)

In this type of diabetes, the level of blood glucose increased in the body of the un-diabetes pregnant mother. Diabetes in pregnancy postures major issues for both mother and baby and has long - term wellbeing suggestions for the child, some of the pregnant ladies with pre - gestational and gestational diabetes mellitus GDM is expanding, basically due to the expanding commonness of corpulence in ladies of childbearing age (Alberti, 1998).

2.1.3 Experimental diabetes

Chimpanzees, primate of non-humans, dogs, cats, rabbits, guinea pigs, hamsters, sheep, rats, mice, bird, fish and other farm animals are the animal using for the purpose of scientific research especially in medical research. Diabetes mellitus animal can be produced by pancreatectomy (Leahy et al., 1994) or feeding or injection or drinking of chemical or antibiotic that causes the diabetic like alloxan and streptozotocin (Szkudelski, 2001).

Animal models have been utilized broadly to concentrate the pathophysiology of T1D and T2D. These models have been important in the advancement of remedial specialists to treat the sicknesses and related difficulties. Rodents, fundamentally mice and rats, are the prevalent creatures utilized as models of diabetes (Peterson et al., 1990; Courteix, 1993). The utilization of these creatures is moderately reasonable and useful. The significance of mouse models has expanded after the presentation of

cutting edge techniques for genetic manipulation, for example, tissue-particular transgenic expression and targeted gene knockout (Mizushima et al., 2010).

2.2. Spinal Cord

Nervous system in the animal and human body is consisted of two mix complex system central nervous system (CNS), which comprises the spinal cord and brain, and the other is peripheral nervous system (PNS) that consist of sympathetic, parasympathetic and autonomic system. Brain and spinal cord are surrounded by bone structure (skull, vertebrate) from outer and inner the membrane envelope (meninges). The bone that surrounded brain its name is skull and the bones that surround the spinal cord its name is vertebrate bone. Meninges membranes are enveloping the CNS. The Meninges encasing the spinal cord comprise of three layers: the furthest dura mater , the middle arachnoid mater and the deepest pia mater (Nicholas and Roy, 1988). Those membranes protect brain and spinal cord from outer mechanical pressure, form these CNS taking the blood and providing a space for the flow of cerebrospinal fluid (CSF). Spinal Cord and meninges located inside the vertebral canal. Spinal cord is the most basic structure between the body and the brain. The spinal cord extends from the foramen magnum where it is consistent with the medullary cone to the level of the 1st or 2nd lumbar vertebrae. It is an indispensable connection between the cerebrum and the body, and from the body to the cerebrum. The spinal cord is 40 to 50 cm long and 1 cm to 1.5 cm in width. These nerve root attaches join distally to frame 31 sets of spinal nerves. The spinal cord is a tube-shaped structure of nervous tissue made out of white and gray matter, is consistently sorted out and is separated into four districts: cervical (C), thoracic (T), lumbar (L) and sacral (S), (Figure 3.1), each of which is involved a few fragments. The spinal nerve contains engine and tactile nerve filaments to and from all parts of the body. Every spinal cord section innervates a dermatome (Nicholas and Roy, 1988).

The spinal string is a piece of the central nervous system, which stretches caudally, it's comprises of longitudinal barrel framework that shipped the flag or beat of sense and engine from fringe of body to cerebrum and the other way around.

The spinal cord controls the willful muscles and which gets tangible data from these locales. The spinal cord in people it involves the upper 66% of the vertebral channel underneath which the vertebral trench contains just the spinal nerve roots and meninges. The normal length of the spinal cord in adult people is 45 cm in guys and 42-43 cm in females, spine is much longer from spinal cord (Figure 2) (Mccotter, 1916). The spinal cord reaches out all through the vertebral trench to the level of fourth sacral vertebra until the third fetal month, after that the vertebral section becomes quicker (Barson and Sands, 1977). In the central of spinal cord one hall present named by central canal. The central canal of the spinal cord extends from base of brain until end of spinal and is lined by a single layer of ependymal cells. The spinal cord is secured to by vertebrae, their related tendons and muscles, the spinal meninges, and the cerebrospinal fluid (CSF). Spinal cord involve two districts gray matter and white matter, the white matter made up of myelinated axons and gray matter contain neuropil, cell bodies, glial cells, neurotransmitters (Yasui et al., 1999).

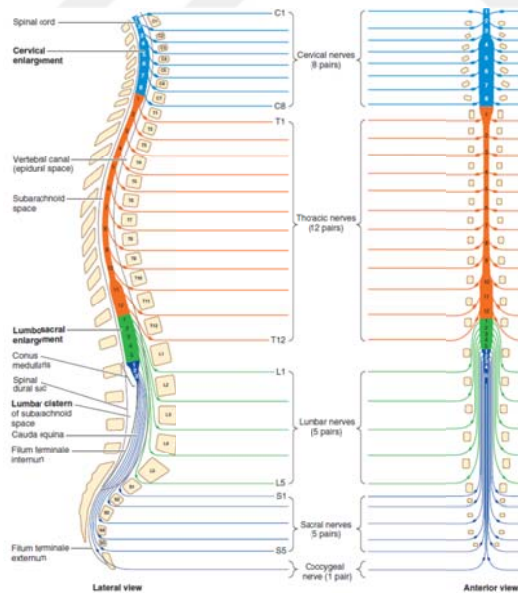


Figure 2. Lateral and medial longitudinal transaction, that showing the spine and spinal cord level of spinal cord segment and vertebral (Moore, 2014).

2.2.1 Embryology of spinal cord

The primary signs of the improvement of the nervous system show up amid the third week as the neural plate and neural groove create on the back part of the trilaminar embryo. The nervous system creates from the neural plate, a thickened territory of embryonic ectoderm. the notochord and paraxial mesoderm actuate the overlying ectoderm to separate into the neural plate (Hockfield and Mckay, 1985).

The improvement of the body of vertebrate developing lives happens in two unmistakable and separate stages. The underlying stage is called primary body development, additionally, is depicted by gastrulation. Amid gastrulation, cells of the epiblast entrance through the primitive streak to build up the three complete germ layers: ectoderm, mesoderm, and endoderm, from which all tissues in the front and the more prominent bit of the body are determined. This is trailed by the following stage called secondary body development (Lawson et al., 1991).

The neuroepithelium thickens and differentiates to form the neural plate. The neuralplate invaginates and thickens to form the neural groove (Lewis and Eisen, 2003), neural tube a cylindrical structure that results from fusion of the edges of the neural groove, enlarges at its cranial end to form the brain (Baldock and Morriss-kay, 2016; Gartner, 2015).

Neurulation, the central nervous system first shows up in the developing life as the neural plate this can be seen at around 18 to 19 days pc (days post-origination) in the human (Figure 3) (Watson et al., 2009; Baldock and Morriss-kay, 2016).

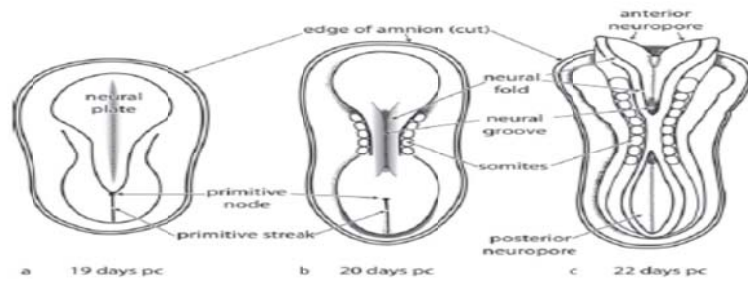


Figure 3. Neural plate and neural tube formation this diagram shows the neural plate and neural tube of human embryos at 18 days pc (a), 20 days pc (b), and 22 days pc (c) showing folding of the neural groove to produce the neural tube. The first point of fusion between the neural folds is at the hindbrain/medulla spinalis junction (Akbarzadeh et al., 2007).

Neurulation a tadpole shaped thickening of the ectoderm rostral to the primitive pit. The following stride is the arrangement of the neural tube, which is the antecedent to the brain and spinal cord, The ectodermal cells just dorsal to the notochord increase in height that mean the cells number increased and differentiated to form a thickened neural plate (Kimmel et al., 1994). The neural plate folds inward (invaginates) to form the neural groove, while the elevations at the groove's open end are called the neural folds. As the groove deepens, the rises intertwine with each other to frame the neural tube (Hodsdon et al., 1992), which isolates from the overlying surface ectoderm and seems to sink into the basic mesoderm.

The future neural crest cells move out of the neural cover as they circuit to twisting up unmistakably the neural crest cells, which now lie between the ectoderm and the neural tube (Schoenwolf and Smith, 1990).

Neurulation this procedure happens in four conspicuous stages despite the fact that they cover both spatially and transiently. (i) formation of the neural plate during which the ectoderm thickens as a result of acceptance; (ii) forming of the neural plate; (iii) bowing of the neural plate; and (iiii) conclusion of the neural groove (and its cranial and caudal closures, the neuropores) with formation of the roof plate of the neural tube, the neural crest and the overlying surface epithelium. The plate is wide at the cranial end, and contracts caudally. Incorporates the change

of the neural plate into the neural tube the incipient embryo at this stage is named the neurula (Schoenwolf et al., 2015). The cranial end will venture into the cerebrum, and even at this primitive stage can be separated outwardly into the fore-, mid-, and hindbrain. The caudal end of the neural plate, which lies over the notochord, forms into the spinal cord (Schoenwolf and Delongo, 1980; Schoenwolf, 1985; Lewis and Eisen, 2003).

Location of spinal cord and positional changes of spinal cord during development after appearing of the spinal cord in the first day in the processing of embryo the position of spinal cord changes in the spine. The spinal cord in the incipient organism broadens the whole length of the vertebral channel at two months (Figure 4-A). The spinal nerves go through the intervertebral foramina inverse their levels of beginning in light of the fact that the vertebral column and develop more quickly than the spinal cord, this positional relationship to the spinal nerves does not hold on. The caudal end of the spinal cord in embryos bit by bit comes to lie at generally more elevated amounts. In a twenty-four week old, it lies at the level of the number one Sacral Vertebra (Figure 4-B). The spinal cord in the neonate ends at the level of the second or third lumbar vertebra (Figure 4-C). In a grown-up, the spinal cord more often than not ends at the substandard outskirts of the main lumbar vertebra (Figure 4-D). Accordingly, the spinal nerve roots, particularly those of the lumbar and sacral fragments, run sideways from the spinal line to the relating level of the vertebral column. The nerve roots mediocre compared to the finish of the cord the medullary cone (conus medullaris) shape a parcel of nerve roots caudal equine that emerges from the lumbosacral augmentation (swelling) and medullary cone of the spinal cord (Figure 4-C and D). Despite the fact that in adults the dura mater and arachnoid mater for the most part end at the S2 vertebra, the pia mater does not. Distal to the caudal end of the spinal cord, the pia mater frames a long, fibrous string, the filum terminale (terminal filum), which shows the first level of the caudal end of the embryonic spinal cord (Figure 4-C and D). This filum stretches out from the medullary cone to the periosteum of the first coccygeal vertebra (Figure 4-D) (Moore et al., 2016).

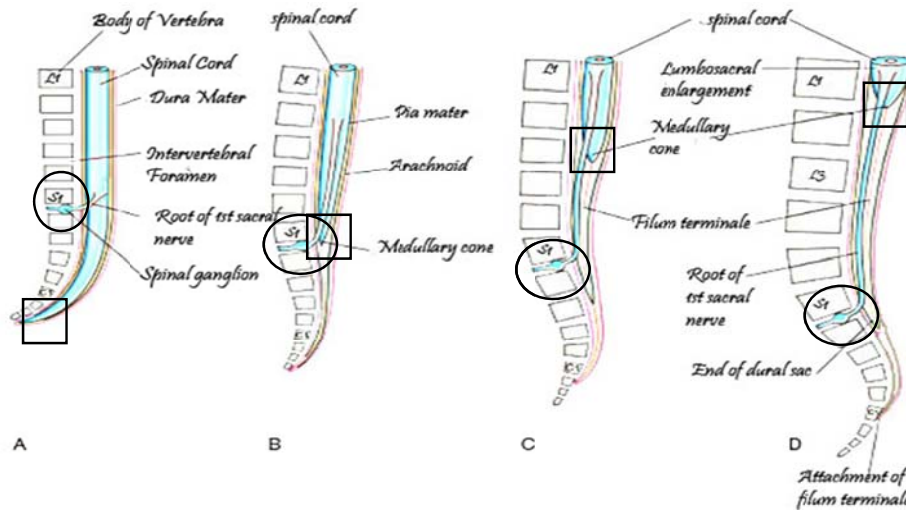


Figure 4. Diagrams showing the position of the caudal end of the spinal cord in relation to the vertebral column and meninges at various stages of development. The increasing inclination of the root of the first sacral nerve is also shown. **A**, At 8 weeks. **B**, at 24 weeks. **C**, Neonate. **D**, Adult. The \square is the Caudal end of spinal cord. The \circ is the Root of the Sacral nerve (Keith et al., 2016).

2.2.2 Anatomy of spinal cord

The spinal cord is the fundamental pathway for data interfacing the brain and fringe anxious system. Spinal cord comparing to length of the spinal column it's too short. The human spinal cord reaches out from the foramen magnum and proceeds through to the conus medullaris bottom of the spinal cord. Close to the second lumbar vertebra, ending in a stringy expansion known as the filum terminale soft threadlike of fibrous tissue (Watson et al., 2009; Heimer, 1983).

The spinal cord is consisted of 5 different locations: the coccygeal, sacral, lumbar, thoracic and cervical segment districts. The cord location different can be seen it by naked eye separated from one another. Two growths of the spinal cord can be envisioned. The cervical augmentation, which reaches out between cervical number three (C3) to thoracic number one (T1); and the lumbar amplifications which stretch out between lumbar number one (L1) to sacral number two (S2) (Clemente, 2011).

The cord is segmentally composed. There are 31 segments areas, described by 31 sets of nerves leaving the string (like a wing) (Figure 5). These nerves are separated into eight cervical, twelve thoracic, five lumbar, five sacral, and one coccygeal nerve. Dorsal and ventral roots (nerve cord) enter and leave the vertebral bit independently through intervertebral foramen at the vertebral bit contrasting with the spinal cord. The number of spinal cord segment compared with spinal vertebrae is same but the length is different, this different return to the embryologic stage development of different tissue (Figure 5) (Clemente, 2011).



Figure 5. The gross anatomy of the spinal cord, gray matter, white matter, and nerve roots (Lennart Heimer, 1983)

The spinal cord is sheathed in an indistinguishable three meninges from is the cerebrum: the pia, arachnoid and dura. The dura is the intense external sheath, the arachnoid lies underneath it, and the pia nearly sticks to the surface of the cord. The spinal cord is added to the dura by a development of sidelong denticulate tendons exuding from the pial folds (Nicholas and Roy, 1988).

2.2.3 Histology of spinal cord

Nervous tissue, made out of upwards of a trillion neurons with huge numbers of interconnections, structures the unpredictable arrangement of neuronal correspondence inside the body. The spinal cord like brain consisted of white and gray matter, the gray matter in the center and white matter around it. Like brain the spinal cord surround by 3 layer of meningeal tissue. Cerebrospinal-fluid surround's the spinal cord and spinal cord and brain are produced from same tissue (Gartner, 2007).

In the central of spinal cord one canal hall present named by (central canal) the central canal of the spinal cord extends from base of brain until end of spinal and is lined by a single layer of ependymal cells (Yasui et al., 1999).

The gray matter has a trademark butterfly or the capital letter H appearance in cross-sections. It comprises of countless and their processes, notwithstanding a significantly bigger number of neuroglial cells. The zenith of the posterior horn, the substantial gelatinous an, is portrayed by an expansive number of small neurons, and one by and large gets the feeling that the neurons increment in size as one moves from the peak of the dorsal horn toward the ventral horn, where the big motor neurons show up (Watson et al., 2009).

On the commence of the social affair of the spinal neurons and their structural attributes, the gray matter of the spinal cord as saw in transverse portion can be detached into ten laminae (Figure 6). Both neurophysiological and neuroanatomical surveys recommend that this cover reflects a relating valuable affiliation (Lima and Coimbra, 1986). A trademark highlight of the gray matter in the thoracic and upper lumbar fragments is the nearness of a lateral horn, in which the autonomic preganglionic motor neurons are found (Heimer, 1983).

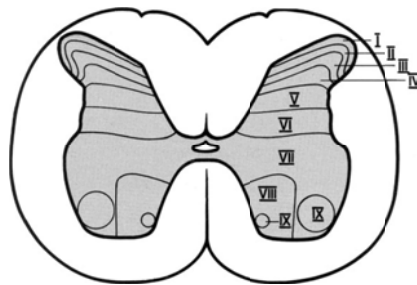


Figure 6. Laminar organization of the spinal cord (Heimer, 1983).

The neurons of the spinal cord are not distributed at random but are gathered together into larger or smaller groups. Usually, the cells within such a group are involved in some common function. The topographical grouping of cells is particularly apparent in the ventral horn; here the motor neurons are arranged longitudinally in columns, the cells in a given column innervating a particular group

of muscles involved in the movement of a joint. It thus appears that there is not a representation of discrete motor pools for individual muscles but rather a functional grouping of muscles acting on a common joint. An afferent volley of nerve impulses (Rexed , 1952).

White Matter is perceptibly distinguished capable in mind and spinal cord areas because of the nearness of myelin that enwraps singular axons and gives electrical protection that encourages axonal conduction of activity possibilities. The high thickness of myelinated axons influences the optical intelligent absorptive properties of white matter (Rastogi, 2007).

In the central of spinal cord one canal hall present named by (central canal) The central canal of the spinal cord extends from base of brain until end of spinal and is lined by a single layer of ependymal cells (Yasui et al., 1999).

2.2.4. Physiology of spinal cord

The greater part of our sensations, sentiments, musings, engine and passionate reactions, learning and memory, the activities of psychoactive medications, the reasons for the mental issue, and whatever other capacity or brokenness of the human mind can't be comprehended without the information about the interesting procedure of correspondence between nerve cells (neurons). Spinal cord has a one of a kind part as a conductor of motivations between the cerebrum and the different peripheral nerves; it likewise serves numerous imperative reflex capacities., The somatic nerves system gives engine driving forces to the skeletal muscles while the autonomic nerves system gives motor impulses to the smooth muscles of the viscera, cardiovascular muscle of the heart, and secretory cells of the exocrine and endocrine glands, along these lines looking after homeostasis (Gartner, 2007).

The most important operational units of the nervous systems are reflexes. A reflex apparatus usually involves a receptor, sensory pathway, modulator, motor pathway and the effector, and the path traced by the reflex action is known as reflex arc (Figure 7) (Rastogi, 2007).

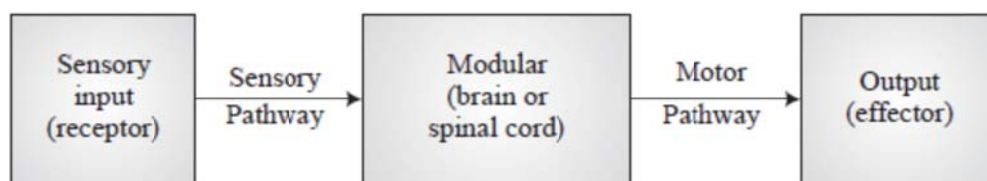


Figure 7. Reflex arc , diagrammatic portrayal of the receptor and effector relationship (Rastogi, 2007).

2.3. T11 Segment

The thoracic spine cord is made up of 12 segments, total between the end one of cervical spinal cord segment and first one of lumbar spinal cord segment. Thoracic eleven is located inside vertebra ten that return to the differential speed growth of them. The T11 segment like all other segment contain sensory, motor, interneuron cells that controlling the muscles, glands in the urinary system and uterus of women and some part of large and small intestinal and sense of this organs, with other segment by producing complex nerve root that coming and going from the spinal cord segment, T11 located in the width part of spinal cord and have width cross-section area that contain a large motor neurons specially in ventral horn, the T11 motor neuron axons reach to urinary system and uterus of women and some part of large and small intestinal (Clemente, 2011).

2.4. Motor Neuron (Motoneurons)

Motor neuron conducts impulses from the central nervous system to other neurons, muscles, and glands. The motoneurons in the spinal cord belong to two functional groups, somatic and visceral. somatic motoneurons innervate skeletal or voluntary muscle while visceral, autonomic motoneurons innervate smooth muscle and glands (Brown, 1981).

Motor neurons present inside the gray mater especially in the ventral horn. The location of motor neurons in the gray matter recognizing by large nuclei (Figure 8) and their appearance in sections stained with silver techniques are so well known (Brown, 1981).

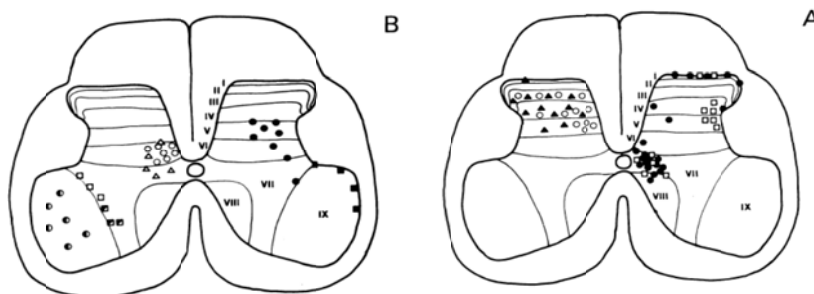


Figure 8. Summary diagrams of the locations of some identified neuron systems. A ▲ spinothalamic tract (cat); ○ neurones with axons ascending the dorsal columns (the postsynaptic dorsal column system); ●, spinothalamic tract (cat); □, spinothalamic tract (monkey). B ○, dorsal spinocerebellar tract (from Clarke's column); ▲, neurones projecting to cerebellum (Aoyama et al. 1973); ■, ●, ventral spinocerebellar tract; □, Ia inhibitory interneurons; ■, Renshaw cells; ●, motoneurons (Brown, 1981).

2.5. Streptozotocins

Streptozotocin ($C_8H_{15}N_3O_7$) or streptozocin or izostazin or zanosar is a normally happening nitrosourea anti-microbial disconnected from the aging results of *streptomyces achromogenes* (Schein et al., 1974). Streptozotocin is a monofunctional nitrosourea derivative isolated from *Streptomyces achromogenes* (Figure 9) (Bolzán and Bianchi, 2002).

Examination of the atomic structure and solidness of the medication recommends that the bond between 2'- carbon and the N-methyl nitrogen might be exceptionally defenseless to scission. Such an occasion would be steady with the watched fuse of the 1- ^{14}C -and 2'- ^{14}C -carbon iotas into basic metabolites and would likewise be perfect with known biological degradation designs for N-nitrosoureido compounds (Lawley and Shah, 1972). The acceptance of test diabetes in the rat utilizing chemicals which specifically crush pancreatic β cells is exceptionally helpful and easy to utilize. As a feature of a review into the digestion system and

method of activity of the diabetogenic sedate streptozotocin (Karunanayake et al., 1975).

The range of the STZ dosage is not as thin as on account of alloxan. The much of the time utilized single intravenous dosage in grown-up rats to actuate IDDM is in the vicinity of 40 and 60 mg/kg (Ganda et al., 1976). Streptozotocin activity in β cells is joined by trademark changes in blood insulin and glucose fixations. Two hours after infusion, the hyperglycemia is seen with an accompanying drop in blood insulin. Around six hours after the fact, hypoglycemia happens with elevated amounts of blood insulin. At long last, hyperglycemia creates and blood insulin levels diminish (Hosokawa et al., 2001; Graham et al, 2011).

Streptozotocin in typical grown-up wistar rats makes pancreas swell and finally causes degeneration in Langerhans islet beta cells and initiates test diabetes mellitus in the 2-4 days (Eastham and Essex, 1969; Akbarzadeh et al., 2007).

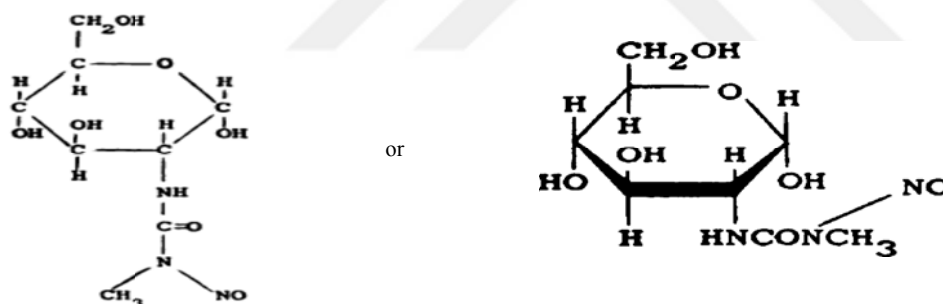


Figure 9. Chemical structural formula of a streptozotocin (Bolzán & Bianchi, 2002)

2.6. Stereological Methods

Stereology is the branch of science that allows interpretation of the three-dimensional (3D) properties of the 3D samples (medical examination, metallurgical samples, biological structures, etc.) based on the data it was received from 2D segment (Mandarim-De-Lacerda, 2003).

Morphologists are customarily inspired by shape and organization of structures in large scale, meso, tiny, and ultrastructural levels. As of late,

morphologists have profited by the utilization of hereditary and atomic strategies to help the comprehending of their issues hence enhancing natural and biomedical researchers. Be that as it may, addresses concerning quantitative adjustments of tissues, cells or cell organelles (which often show up in adjustment, advancement or pathology of a life form), and in addition, a superior connection amongst's morphology and capacity, require a quantitative way to deal with being surely knew (Andersen and Pakkenberg, 2003).

If the sections are considered as planes passing through any structure and intersecting the components of the structure, each component of the structure forms projections (profiles) in these sections in relation to the number, size and coverage of the length, area and volume ratio. These projections are additionally used to get data about the segments included. However, the projections of the components contained in the structure in the sections are merely representations on the plane of section of the structures they belong to. Therefore, making direct interpretations from these projections can be quite misleading because of the lack of real data on the three-dimensional properties of their components (Figure 10) (Kaplan et al., 1997).

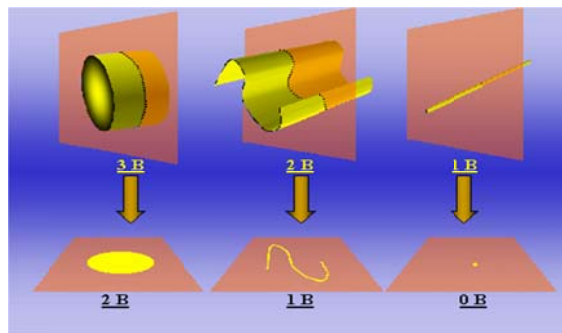


Figure 10. Size reduction in specimens made with two-dimensional sections. The number can only be sampled with a three-dimensional sampling probe (Weibel, 1969).

For example, contained within the "structure" of the type of particle (eg, neurons in the brain), we want to determine the number, we directly "a" cannot make a presentation of the sections taken on the two-dimensional structure containing particles. Because the expectations on them in parts of particles, their size,

segmented perpendicular to the extension direction, size, etc. .. is closely related to these factors. Larger particles, while the chance of cutting more likely a plane section than a small, the small particles has fewer expectations than chance (Figure 11) (Kaplan et al, 1997).

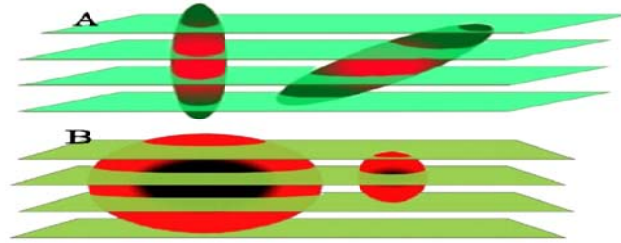


Figure 11. Effect of particle size and orientation on sampling chance. This can only be done by three-dimensional sampling strategies (since Gundersen was modified from 1992), since two-dimensional sections contain such misleading information.

The cross-sectional direction is influential in the sampling of the particles in relation to the particle orientation. In Figure 12, the effect of the segmenting direction on the chance of sampling the particles is schematized. As can be seen, the sections with equal spacing are more when taken in a direction perpendicular to the long axes of the particles; when parallel is taken; fewer projections are obtained from the same particles. On the other hand, all particles, regardless of orientation, should have equal chance of sampling, since each particle counted as "1" when viewed from the viewpoint (Kaplan et al., 1997).

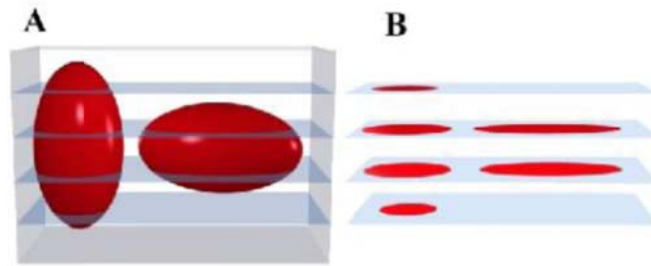


Figure 12. The relationship between the direction of equally spaced cross-sections through a volume with the inclusion particles co-orientated (showing an aspect across a certain direction) and the chance of sampling the particles in the volume. In A, perpendicular to the particle orientation, and parallel to B, the sections are schematized (Gundersen, modified from 1992).

Essentially, the expression "section" alludes to planes going through any strong structure and not having a thickness ($t = 0$). As a decent case, a cut and cleaned surface of a metal example can be given. Since the mine examples are not light-impermeable, an eyewitness looking at these examples confronts a genuine two-dimensional plane relating to the cleaned surface. Be that as it may, the segments taken from organic examples are really cut with a specific thickness. Regardless of how little their thickness, they cannot be specifically considered as two-dimensional planes. Therefore, the sections taken from biological specimens, whether for light or electron microscopy, are not considered in terms of their thickness. The premise of stereological strategies is the "Systematic Random Sampling" (SRS) system. The fundamental element of this testing arrangement is that each purpose of the structure has the shot of being examined consistently when it is important to take tests from the structure to be contemplated (Pakkenberg and Gundersen, 1988).

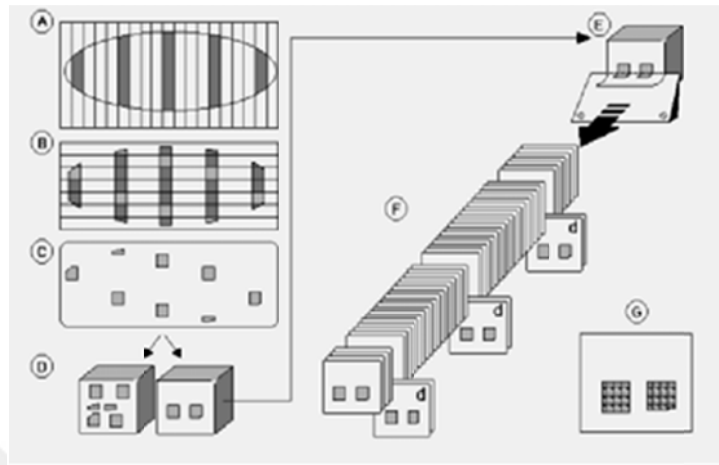


Figure 13. Schematic representation of the physical fractionation method. The total number of particles is calculated by multiplying steps the number of total discrete particles by the inverse of the disintegration ratios in all sampling (Canan et al., 2002).

Biological constructs are often too large for their components to be examined and inspected by the investigator (cell, nucleus, vesicle etc.), so it is practically impossible to include all the cross-sections obtained from the construct into the study. Notwithstanding, for a study to determine the total number of neurons in the human neocortex, tens of thousands of histological sections from brain to be studied cannot be examined individually. In this case, it is necessary to make a selection among the possible samples (sections) that can be obtained at certain ratios. When making this selection, it is a statistical requirement that each point of the structure has the chance of equal sampling so that the selected samples can represent the best way of doing so. Randomly choosing to provide this condition does not exactly solve the problem. Here comes the preeminence of the SRS here. The SRS includes sampling the entirety of the structure of interest, starting at a random point within the first interval, over a predetermined fixed sampling interval. If the predetermined sampling interval (e.g., the series of the first ten slices when deciding to select each tenth slice or part), the systematic part of the sample should be started at a random point within the first interval (e.g., by selecting any of the first ten slices as the start, (Figure 13) (Kaplan et al., 1997).

The number of particles (molecules) determination of the numerical intensities (N_v) of the total number of particles or units of the biological constituents, in the biological constructs is an indispensable parameter for many studies. In the nervous system, the numbers of the nerve cells, which are the basic functional elements, are frequently mentioned as important data in researches. For many research topics such as the number concept interpreted as an important expression of structure and function, the development of organs, periodic function changes, effects of chemical substances and physical treatments, adaptive specialization, learning and memory, mechanisms of disease formation and aging, Is one of the research data on which comments are made. Although the number concept is so important, it has not been possible to provide a method to keep the particle counts within an acceptable margin of error for many years (Kaplan et al., 1997).

To make grain counts, it is necessary to take the sections of the structures we are interested in. However, these sections are two-dimensional images that cannot exemplify the concept of a zero-dimensional number distributed only in a three-dimensional environment when viewed as images. The attempt to reach the number of particles by direct counting of the expectations of the particles in the cross-sections is one of the first attempted methods. But it has not taken a long time for researchers involved in counting to realize that the number of projections and the number of particles are not directly related. The number of particles is a zero-dimensional quantity that should be sampled independently of three-dimensional effects such as the size or orientation of the grain. It is zero size, because; Regardless of the dimensional characteristics (size, length, diameter, volume, etc.) of any of the birds, it is a value one when the number is the word. That is, the number is independent of the dimensional properties. However, the sections obtained from the structures are regarded as two-dimensional planes and the particles are sampled in a manner closely related to the dimensional properties. The series and equally spaced sections passing through a structure are larger than the ones with large grains settling in parallel to the direction of sectioning (Figure 10-12). That is, the chance of a bee getting hit by a section depends on the size, height, and orientation of the bee (Kaplan et al., 1997).

Though the sections are regarded as two-dimensional planes, their thickness must be taken into account as they are slices with finite thickness. If the thickness is neglected and the sectional images are considered as two-dimensional planes, the effect of the thickness on the number of particles may cause a counting error. As the cross-sectional thickness increases, the frequency of appearance of the particles within the cross-sections will increase. Since the histological sections are transparent, this increase occurs as an increase in the number of expectations (Figure 13). The expectation (formerly known as the Holmes Effect) is called the over-expectation due to the thickness of the cross section. After recognizing the Holmes effect, researchers have tried to overcome this problem using many correction factors. The most famous and perhaps most popular of these is Abercrombie's correction factor. In his famous work published in 1946, Abercrombie focuses on the counting errors that occur due to the cross-sectional thickness and particle size. Accordingly, the actual number of particles counted; the number of particles or particles obtained in the counting must be equal to the product of the cross-sectional thickness / (cross-sectional thickness x particles height) and a correction factor. This statement is formulated as follows;

$$N = \frac{\sum Q}{h \cdot \sum a_{(frame)}} \cdot V_{(ref)}$$

Here; N is the total number of particles; Q is the number of discrete particles; H is the distance between the sections (i.e., the height of the divider): $a_{(frame)}$, the area of the neutral counting frame used in the count and V (ref) is the total (or reference) volume of the structure being studied. In this case, for example, if the slice thickness is equal to or close to the average grain height, the actual number of grains will be approximately half of the number of grains obtained as a result of the count (Abercrombie, 1946).

2.6.1 Disector

Disector; was first described by Sterio in 1984 (Sterio is a nickname for a famous "Viking" stereologist, who is an anagram of the word discipline, which has had great contributions to stereological methods and is still working on this subject).

This method can also be described as a virtual 3D stereological investigation used in particle counting. The disector's basic rationale is to find the "ends" of particles, i.e. particles, where particles first appear or are seen last along the direction of sectioning. A method that works with this logic, if it is thought to be a single entity in one direction, regardless of the shape and orientation of each of your creatures, can achieve the actual number of particles (Kaplan et al., 1997; Altunkaynak, 2012).

2.6.2 Physical disector:

It is the first appearance of the disector. In this method, two consecutive or separated sections separated by a certain distance from each other are taken and counted as particles not found in the other. The distance between the two sections is referred to as the "height of the disector" and the number of detector particles that can be sampled along the height of the disector, i.e., the number of particle edges, is found at the end of the count. This gives the numerical density (N_V) of the particles studied (Kaplan et al., 1997).

Disector is in the form of a comparison of the basic application, taking two sections with a distance less than the minimum particle height. The requirement that the cross-section distance be less than the minimum particle diameter is intended to ensure that the particles are not skipped between the cross-sections without being cut off (i.e. without being sampled). When a single particle is hit by a section, it depends on the height of the particle in the cross-section direction; the chance of "being cut by a section and not being cut by consecutive parallel" is equal for all large and small particles. By this way of connection, the total number (or numerical densities) of particles in a given volume can be calculated;

$$N = \frac{\sum Q^-}{h \cdot \sum a_{(frame)}} \cdot V_{(ref)}$$

Where N: is the total number of particles; Q^- : is the number of discrete particles; h: the distance between the cross-sections (i.e., the height of the disector); $a_{(frame)}$: denotes the field of the unbiased counting frame used in the count, $V_{(ref)}$ denotes the total (or reference) volume of the structure being studied. If the value of

$V_{(ref)}$ is to be subtracted from this form, the resulting value will be the numerical intensities of the particles - not including the total volume of the account. However, in most cases, the numerical intensity value does not directly provide information on the change in the total number of particles, so it may be objectionable to use this value in comparative studies and to make biological interpretations accordingly (Kaplan et al., 1997).

The detector particle is the name given to the particles that can be counted during the counting done by the discrete method. In the physical disector, one of the cross-sectional pairs taken for counting is used as the reference section and the other look-up section. These sections are examined and the sample is found in the sample section, and the particles which are not in the observation section are counted as the discard particle and are indicated by the symbol "Q-". These are the particle tips that can be sampled in the height of the detector (Figure 14) (Kaplan et al., 1997).

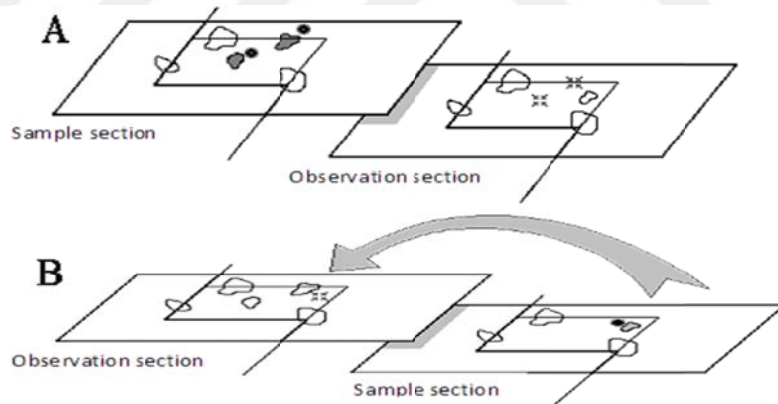


Figure 14. Schematic representation of physical discrete application. One of the sections is called the sample and the other is called the observation section, and the particle projections, which are not found in the observation section, are counted as the discrete particles (Q-) (A). In order to increase the number of detector samples, a two-way discrete count can be applied by changing the roles of the sections (B) (Ünal et al., 2002)

During the disk counting, sample and observation sections, changing their roles, that is, section observation used as sample section; the observation section can

be evaluated as a sample section, and a two-way counting can also be performed. This makes it possible to increase the number of discretized sections without needing additional cross-sectioning, and thus to be able to work on more samples (Figure 14) (Kaplan et al., 1997).

As a result of counting by the detector method, the reference or total volume must be known so that the total number of particles can be obtained. The particles of the structure to be counted can be calculated by different methods depending on the properties of the structure. (Kaplan et al., 1997), it is easy to find that the working structure has as much volume as the amount of water it carries, by immersing it in an isolated, macroscopic (e.g. whole T11 segment) dimension.

But if the structure studied is an organization that cannot be isolated from the surrounding structures, such as a brain nucleus, a lymph follicle, or a tumor, then the Cavalieri principle can be used to calculate the volume (this principle is referred to as the Italian mathematician who first introduced his mathematical foundations). According to this principle, the structure for which the volume is to be calculated is divided into serial sections from the beginning to the end. The area of projections belonging to each structure is calculated. Area calculation can be done using costly image analysis systems or using a dotted area measurement chart to achieve the same reliability results. Field measurement rulings are patterns consisting of points, each of which represents a certain area. The area of interest of these structures can be easily calculated by randomly casting the cross-sectional images or the area on a surface to be calculated and counting the points falling within the relevant area. When the total number of dots falling into the area is multiplied by the area represented by each dot, the area of the corresponding area is obtained. So;

$$A = \sum p \cdot a(p)$$

Where P is the number of dots; a (p) represents the area represented by a single dot on the section (Kaplan et al., 1997).

After calculating the area of the image of the obtained section, the product of the average section thickness and the total area gives the total volume of the structure

concerned. This calculation can be done by taking the sum of the individual volume values (area X thickness) for each section after the calculation, or by multiplying the field values by the average sectional thickness, as the case may be. Generally, microscopic field calculations are performed while the second method is more practical (Kaplan et al., 1997).

2.6.3 Counting frame

In situations where grain projections are used to make grain counts, the grain projections that appear in the sections need to be limited to a certain area and counted. In this case, the question arises as to which rules should be used to limit projections. In the classically applied old methods, a frame in a square or rectangular structure is a widely used method of counting particle projections falling directly into this frame, on projections. Then, when it turns out that this type of count causes the number of particles to be overestimated, a simple counting frame, which is divided into two along one of its diagonals, has begun to be used (Figure 15). If the count in this frame is a rule, counting the particles that hit one half of the frame edges and not counting the other half are counted. But it is understood that this frame is far from giving the actual grain value, then the emergence of the frame of unbiased counting. The reason for this type of counting mistakes resulting from the counting frames is explained by an effect called "edge effect". Briefly, the edge effect emphasizes the question of which rules should be used to judge particles intersecting frame edges when there is no problem counting particles falling into the frame when any counting frame is used (Kaplan et al., 1997).

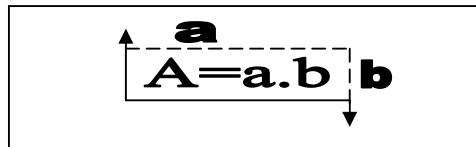


Figure 15. Counts frame (Gundersen 1977).

The neutral counting frame is, as most commonly used, a simple rectangle with four corners symbolized by two types of lines: thick and flat, and thin and slender. Although there are not many changes in appearance, counting rules are

different from other counting frameworks. Basically, the edges are "inclusive", including thin and dashed lines, and "out" or "forbidden" edges are continuous lines. That is, while the projections that correspond to the cut lines are counted, the projections that hit the continuous lines are excluded from the count. The most important feature of the counting frame is the extensions of prohibited edges. These extensions are extended to cover the entire image area in which the frame is placed. The counting frame is the most efficient and reliable counting framework currently available for grain counting. It is also proven by geometric calculations that this frame provides the most accurate count of particle projections (Gundersen and Jensen, 1987).

2.6.4 Measuring cross-section thickness

The section thickness is important in calculating the number of particles. In methods other than physical fragmentation, in order to reach the number of particles, the volume value to be counted must be known. The value of volume requires that the counting area and the counting "thickness" be known (Kaplan et al., 1997).

The cross-sectional thickness is important in electron microscopy as well as in light microscopy. Although many methods are used to measure section thickness, only the method used in the study will be discussed (Kaplan et al., 1997).

For the application of stereological methods, the distance traveled by the microscope table in the vertical axis (z-axis) is generally calculated during the change of the focus to measure the cross-sectional thickness (light microscope). This distance variation is usually accomplished by means of graders on either the microscope micro or macro screw or by means of a microcontroller mounted on the microscope table and sensitive to the movements of the table in the vertical axis. However, the ratings on the microscope screws are not very sensitive due to the backlash between the opposite directions of the screws, and cannot always be reliably used. However, by expanding the scales on these screws, a safer measurement can be achieved (Kaplan et al., 1997).

Electronic or mechanical microcontrollers are much more precise measurement tools. As previously used mechanical types are still available, those that are more widely used electronically are now being used. The electronic microcontroller consists of a digital display and a motion sensor. Vertical position changes detected by the motion sensor on the microscope table are read at micrometer (μm) level from the digital indicator of the microcomputer. Generally, digital microcontrollers are $0.1 \mu\text{m}$ sensitive (Kaplan et al., 1997).

When a cross-sectional thickness or a thickness within the cross-section is determined by means of a microcatcher or a similar device, the lower and upper surfaces of the cross-section must be determined by the investigator in different levels of focus. The microscope image is the upper face of the section where the first clear view is obtained when it is approached to the upper surface of the section; if the final image is the clear image, the bottom face of the section. Moving up or down the microscope table while optically advancing between these two, will give the cross-sectional thickness (Kaplan et al., 1997).

2.6.5 Fractionation

Fractionators are an examining plan joined with a stereological estimation bringing about an unbiased estimate of the aggregate amount of interest. For the fractionators, an extrapolation is done to reach a gauge (Altunkaynak, 2012). The method of splitting in stereology is currently the most commonly used method of particle counting (or calculating area, volume, length, etc.) of stereology. It is one of the most preferred methods (Kaplan et al., 1997), in that it is not affected by any shape changes in the tissue, it does not need values such as cross-sectional thickness, shrinkage-swelling amount and is a highly effective method (Dorph-Petersen, 2001).

The principle of fragmentation is to perform particle counting on a relatively small piece of tissue selected from uniform, systematic random sampling from any structure. The only requirement is that the amount of tissue sampled for counting is how many times the original design corresponds to what is known as the ratio to the main structure. The number of particles obtained from this small tissue section is used only when this small fraction is multiplied by the ratio to the parent structure to

obtain the total number. Since there is only a sampling rate in question, there is no need to make any preliminary assumptions about the slice thickness, deformation grade and texture. The fragmentation method is so simple, objective and efficient that it is not known how to make a biased fractionation (West et al, 1991; Kaplan et al., 1997).

The fragmentation method is actually a sampling plan rather than a particle counting method. This resultant method, which involves counting according to the discrete counting method rules in the tissue sampled by the fragmentation method, is divided optically and physically into two types according to the type of the discrete application used in particle counting. The basic logic is the same in both methods, but there are some differences in practice (Sterio, 1983; Kaplan et al., 1997).

2.6.6 Physical fractionation:

Physical fragmentation is a component of the fragmentation sampling and physical disector counting method. Although implemented basically by the same mechanism, there are a number of application differences with optical fragmentation. In terms of its application, it cannot be used in some cases, but the same is true for the method of optical disruption (Kaplan et al., 1997).

Physical fragmentation can be summarized by sampling the particles, which are to be counted, by separating smaller physical fragments with certain steps, and by obtaining the total number of particles from certain fractions as a result of the latest sampling. At the basis of the fragmentation method is the systematic random sampling logic. The only condition to be observed in the samples taken at various stages from the working structure is the systematic and random sample selection; That is, a random start sample is selected from the range including the first samples, and then every sample following this selected sample must be sampled. Where is the predetermined sampling interval (if the decision is made to select one of every 20 sections, 20 ones) (Kaplan et al., 1997).

Another feature of the physical disector method is the stepped sample. At each step, a sampling is done systematically and randomly in a known manner, from

the examples that are needed. In the next step, a new sampling is performed from the selected samples in the previous sampling step. In each sample, it is necessary to know how much of the selected parts or a section corresponds, for example, to the structure or samples taken. This value is called the fractionation factor and is indicated by "f" (Kaplan et al., 1997).

The main purpose of the shattering method is to obtain results within a certain and acceptable margin of error on a piece that corresponds to a certain proportion of the work being worked and as small as possible, as in all stereological methods. If the method is unbiased by nature, as the number of samples increases, it will be possible to obtain closer results with real values. Therefore, in order to obtain results within a predetermined error margin (usually less than 10%), the variable with the greatest effect on the error coefficient should be determined during the preliminary operation. A preliminary study on at least 5 animals is sufficient to determine the error rate and the contributing factors. A preliminary study on a single animal cannot give an idea of the suitability of the work plan because as a general rule the greatest contribution to the variability of results is always from the differences between individuals (from biological difference). To add this to the account, the first thing to do is to start with a preliminary study that can reveal the differences between individuals. If the desired error coefficient is achieved, sampling can be done easily at each step (Kaplan et al., 1997).

In the physical disector method, the working structure is subjected to a series of disector sequences. After recording the proportions of systematically and randomly selected fragments in each step, the last remaining fragments are embedded in the blocks and divided into sections until the end. Systematic and random samples are taken from these sections. Then, while cell counting is under the microscope, sampling can be done among the counting areas (Figure 13). The only requirement is to know the "fragmentation rates" of these sample selections, which are systematic and random. The number of particles obtained as a result of the particle count performed after all the samples are made indicates the number of particles in such a portion of the work being worked. This number is multiplied by

the inverse of the sampling rates, and the total number of particles is calculated. This process can be briefly formulated as follows:

$$N = \frac{1}{f_1} \cdot \frac{1}{f_2} \cdot \frac{1}{f_3} \dots \frac{1}{f_n} \times \sum \bar{Q}$$

Where $f_1, f_2, f_3 \dots$ and f_n denote the fractionation rates. In the first sample, if one of every 5 slices of a sliced structure is taken, $f_1 = 1/5$. The product of the total number of divider particles ($\sum Q$ -) multiplied by the inverse of the fractionation rates recorded in all steps will also give the total number of particles counted (Kaplan et al., 1997).

As can be understood from its basic logic, the method is completely neutral. There is no need for any preliminary acceptance of the structure being worked on, nor does it require any other ratios (slice thickness, deformation constant, etc.) other than fragmentation rates. When applied correctly, the greater the number of samples, the closer the actual value is calculated. The sampling of the particles by the method of disintegration depends only on their physical existence. So they are sampled if they are, otherwise they cannot be sampled. All of the existing particles have equal chance of sampling. Moreover, it is one of the most effective methods since it enables to obtain results within the desired variability limits in a very short time by working on very small sample (Kaplan et al., 1997).

2.6.7 Pointed area measurement scale

The projected surface areas of the structure of interest are calculated on the surfaces facing the same direction of the sections, and the resulting "total surface area" is multiplied by the average section thickness, thus obtaining an objective calculation of the total volume of the structure in the examined cross-sectional images. For field calculation, the simplest and unbiased method is to use a dotted area measurement ruler. The dotted area measurement scale consists of systematic + marks representing points separated equally by each other (Figure 16). Each dot represents a unit square (d^2) when there is a constant interval (d) between marks. This unit is known as a square or quadrilateral, 'dot related area' [$a(p)$]. The extent to

which many such points from such a ruler, randomly placed on an image, will hit the image of interest depends on the size of the cross-sectional area and the distance between the points. A fixed point, identified in each of these increments, is used for counting (Canan et al., 2002).

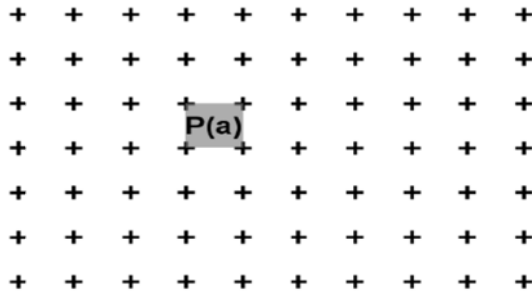


Figure 16. Example of a dotted area measurement ruler.

The figures on the images of the area of interest are counted from the points in this chart which are deployed randomly on the cross-section view. The area (A) of the section view can be calculated by multiplying the total number of falling points (Σp) by the area represented by a point [a / p].

$$A = \Sigma p \cdot [a(p)]$$

It has been shown that the calculations made with the above mentioned method do not show any difference in accuracy and accuracy with the calculations made with the advanced image analysis systems (Gundersen et al., 1981).

2.6.8 Application of disector cavalieri

An application that yields a total number of objects by removing the cut-off thickness measurement from the center is the combination of Cavalleri and the dis-charter designated by Pakkenberg and Gundersen in 1988. The essence of this application is based on the fact that the object density (Nv) and the reference volume (V_{ref} , volume of the structure in which the objects are located) are obtained from the same sections. As a result, the total number of particles (N) is obtained by multiplying both;

$$\mathbf{N} = \mathbf{N}_V \times \mathbf{V}_{\text{ref}} \quad (1)$$

Since both parameters are obtained from the same cross-sections, the tissue deformation and the cross-sectional thickness that they have are the same for both. In the latter process (during the calculation of N) one share will take the same cross-sectional thicknesses in the other pie (Gundersen et al., 1988).

As you can see, this combination is achieved in two stages (N). For this purpose, the structure to be investigated is first turned into sections and all the cross-sections are taken with SRS. As mentioned earlier from these cross-sectional pairs, the N_V with the divisors is calculated;

$$\mathbf{N}_V = \frac{\sum \bar{Q}}{\mathbf{t}} \times \sum \mathbf{a} \text{ (frame)} \quad (2)$$

The volume of the build (V_{ref}) is calculated using a cross-section of each cross-section. The volume calculation is based on the Cavalieri method. As will be remembered, this method is capable of multiplying the total profile areas of the volume (t) of any structure by the cross-sectional thickness (t);

$$\mathbf{V}_{\text{ref}} = \mathbf{t} \times \sum \mathbf{a} \text{ (profil area)} \quad (3)$$

It is not necessary to use all sections in this volume calculation. It is enough to use every (k.) Section. In this case Equation - 3 takes the form.

$$\mathbf{V}_{\text{ref}} = \mathbf{t} \times \mathbf{k} \times \sum \mathbf{a} \text{ (profile area)} \quad (4)$$

The cross-section areas in the sections can be determined very quickly and efficiently with the dot count. This is done by using probes containing systematic test points. Each point (P) in the probe represents a certain area, a/p. Such a probe is randomly dropped on the profile, and then random points (P) are counted on the profile. When the total number of points is multiplied by the points represented by each point, the profile area is calculated (Gundersen et al., 1988a);

$$\sum \mathbf{a} \text{ (cross-section area)} = \mathbf{a/p} \times \sum \mathbf{p} \quad (5)$$

When these values of the profile field are substituted in Equation - 4, the equality returns as follows;

$$V_{\text{ref}} = t \times k \times a/p \times \sum_p \quad (6)$$

Equation 2 giving (N_v) and Equation 6 giving (V_{ref}) would be put at places in Equation-1

$$N = N_v \times V_{\text{ref}} = \sum \bar{Q} / t \times \sum a \text{ (frame)} \times [t \times k \times a/p \times \sum_p] \quad (7)$$

With this equation, if the average number of objects in the (a) the sigline is reduced.

$$N = \bar{Q} \times \sum_p \times k \times \frac{(a/p)}{a \text{ (frame)}} \quad (8)$$

As you can see, the intersection height does not have to be known according to this last equality in which (N) is obtained. Note that this calculation pattern is not affected by the tissue deformation during the follow-up and cross-sectional retrieval. Because none of these will affect the ratio of the areas defined in the same sections [a / p] / a (frame). Furthermore, the deformations that occur in the tissues in comparable groups do not have to be equal (Gundersen et al, 1988).

3. MATERIALS AND METHODS

3.1. Materials

All conventions were reviewed and approved by the Yuzuncu Yil University animal care committee responsible for animal care guidelines under number TYL-2016-5507 in 12/13/2016. All principles of laboratory animal care were strictly followed. We conducted our laboratory study at the stereology-laboratory of Histology and Embryology department at Faculty of Medical.

We have used twenty-eight male rats of Wistar albino rat, which were adult's rats at (4-5) weeks of life. These rats have lived and grew up in the experimental animal's unit house were housed in cages metabolism under environmental conditions controlled by the 18-25 °C and (12-hour light/dark) cycle. The rats fed a uniform pallet and tap water with free nutrition (Figure 17).



Figure 17. Cages in which the animals are housed.

3.2. Application of Experiment

To perform the work we used the rat as the experimental animal because it easy to work on them. The genes of rats are very close to human genes. Have the same anatomy and physiology with a very slight difference. The cost of work on rats is inexpensive compared with other animals.

In the first day, we given it the number as a name that wrote on the tail for all rats after divided into 4 group; 7 number in the control group (I), 7 number in the saline group (II), 7 number in the 45mg/kg of STZ group (III) and 7 number in the 65mg/kg of STZ group(IV). Prior to the experiment, weights of all experimental groups were recorded and tabulated (Table 3) weighing between (152-256) g. In second day of work, after stopping feeding for 12 hour, took blood from tail of all rats by pinprick (Figure18-a) to examination the level of glucose in blood by used blood glucometer (Figure 18-b), were recorded tests, all groups (II, III, IV) injected intraperitoneally (Figure 19), group (IV) by the 65mg/kg of STZ, group (III) by the 45mg/kg of STZ and group (II) by 0.5ml of physiology saline 0.9%, while control group was not injected. The 45mg/kg is the lower dose, and 65mg /kg is the higher dose for the human body (Graham et al., 2011; Deeds et al. , 2011).

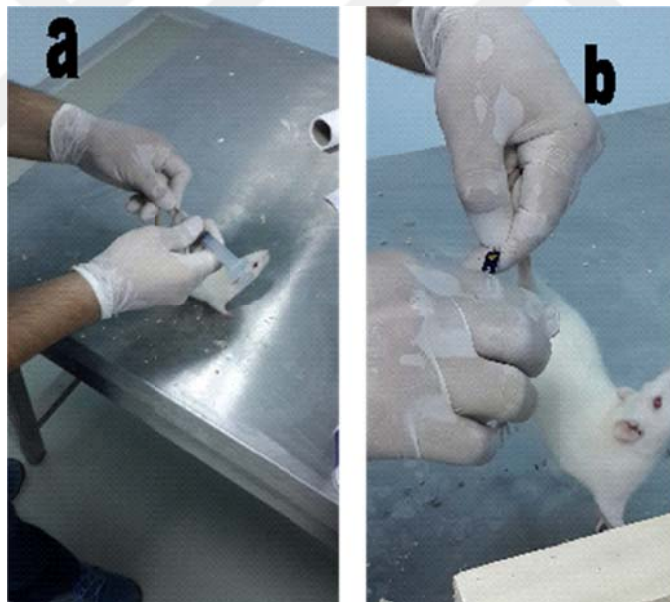


Figure 18. a-Tacked blood from tail of all rats by pinprick, b-The used blood glucometer.

After 4 days of injection again, weights of all experimental groups were recorded and tabulated (Table 2). In the sixth day of work after 12 hours of stopping feeding tacked blood again from the tail of all rats were recorded and tabulated (Akbarzadeh et al., 2007).



Figure 19. Right intraperitoneally injection.

We recorded the glucose level in blood of all rats for each group on table separately. At the end, in the seventh day, animals were perfused. The animals were anaesthetized by used insulin syringe to pushed ketamine (50mg/kg) as anaesthesia drugs to left part of rat abdominal-peritoneal, after the rat were anaesthetized we used toe- pinch-response method to determine a depth of anaesthesia, after the animal not responded the incision process was performed by opened the abdomen and removed the thoracic diaphragm. Used 3 ways stopcock cannula with extension tube end needle, that penetrated the left ventricle to pushed perfusion drugs to the circulatory system. Pushed of heparin (0.5 cc), at the first to prevent blood clotting in artery and vein of the body. And right atrium was opened by incision to take out the blood. Physiological saline 0.9% was administered intracardially with the aid of a cannula until the color of the blood was clear then; the areas related to 10% neutral buffered formaldehyde were perfused for 5 to 10 minutes until bleaching (Figure 20).



Figure 20. Perfused process until bleaching.

The animals were sacrificed under anesthesia, the rats remained in a 2.5% of glutaraldehyde for (24-48) hours. The T11 vertebra was removed by the thoracic vertebrectomy, we tacked the samples from the rats by scalpel blades, after opened the abdomen of rat removed the thoracic diaphragm (Figure 21-a.). Under the lung and heart, cut the ribs number 10 (left & right) of vertebra number (10) in the location that join to the vertebra (10), superior border of vertebrae (10), and the superior border of the vertebra (11) from the vertebral column. Excised the sample, separate the bone vertebra (thoracic vertebra T10 that contained the T11 segment of the spinal cord of the rats) (Figure 21-b.) (Moonen, 2014; Moonen et al., 2016).

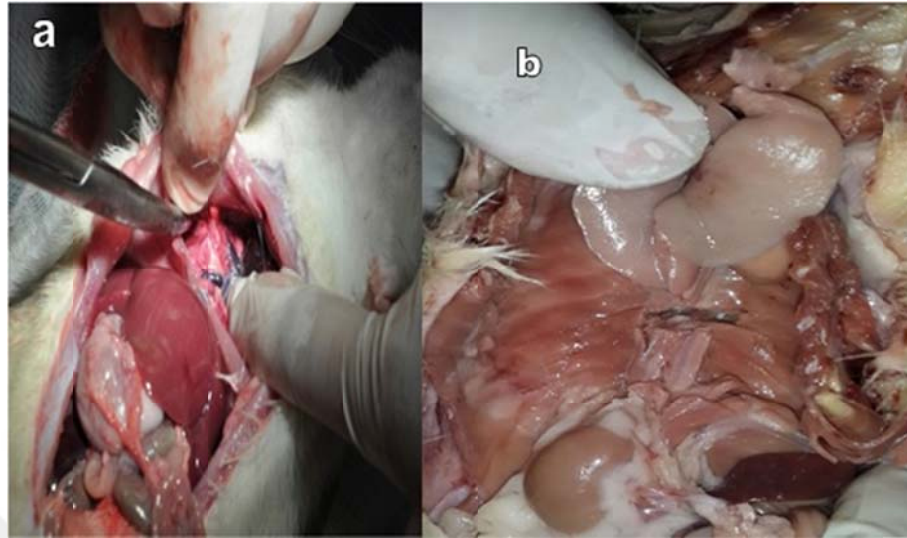


Figure 21 a- Removed the thoracic diaphragm, **b-** Vertebrectomy.

The T11 spinal cord segment take out inside the thoracic vertebrae bone and only (2 mm) of spinal cord was took (Figure 22), Putting the all samples in the four different (eight Division Small Disposable Baskets) and by (Basket stem assembly) to gather holding, Immersed the samples in the buffer solution osmium tetroxide (OsO₄) in a (Disposable Vials 20 ml), by (parafilm) covering the head of vial, The samples remain in OsO₄ at (4 °C) for (1:45) hours as the another step proses of fixation (Ayrancı et al., 2013).

Next step the dehydration of sample tissue performed by immersed the sample in the series and different concentration of alcohol (ethanol) from low concentration to higher concentration (50%, 60%, 70%, 80%, and 98%), after propylene oxide those pieces samples embedding in the (epoxy resin) in the (TEM multi-well embedding mold) every sample separately was recorded as a sampling rate of 1/1 (f1) in one template (Figure 22) and remained in the Incubator at (60 °C) for (24) hours to become solid blocked with Epon (Kua et al., 2016).

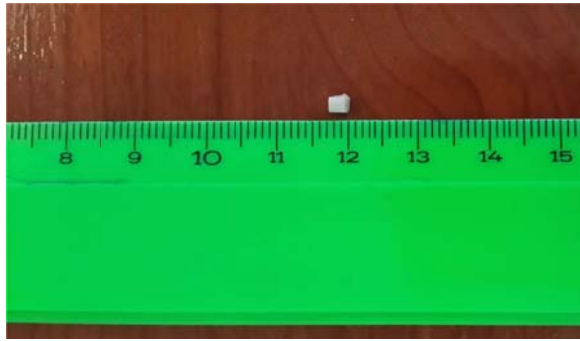


Figure 22. The T11 spinal cord segment 2mm.

The Transmission Electron Microscope-Preparation Specimen technique was used to obtain 5-slides, from each rat sample. The parallel and serial sections at equal distances of 1 μ m thickness (Figure 23) from the constructed blocks were taken at 1/100 (f2) (Cross-sectional sampling share). Because the counts to be made are made by physical disector method, the consecutive parts of each selected section were taken together to form pairs of disciplines. These sections were stained with modified borax toluidine blue stain. "Zeiss axioskop 40" model light-microscope was used. The photos were taken at 40X lens magnification.

Volume ratio was measured with dotted area ruler using the modified method of Cavalieri's principle. Volume was calculated with the help of "SHTEREOM 1.5" ready pack program.

$$V = t \times a/p \times \Sigma_p$$

V: is the volume of the object (motor neuron) of interest in the slice plan, T: Section thickness, a/p: Area between two points, Σ_p : Total number of points cutting section.

After calculating the volume values using the above formula separately for each rat, total motor neuron area volume was reached with the following formula.

$$\text{Total Volume} = V_1 + V_2 + \dots + V_n$$

V1: volume of section 1, V2: volume of section 2, Vn: n. Sectional volume

Estimation of number motor neuron, using a "Zeiss axioskop 40" model light microscope, photographs was taken at 100X lens magnification (Figure 23). Disector-Cavalierly application was used for numbers of the motor neuron was calculated with the counting frame. From the cross-sections obtained from each animal; the total number (N) was calculated by multiplying the number of the resulting disector particles (\bar{Q}), the number of points in the total volume calculation (Σ_p), the cross-sectional thickness (k), and the dot area (a/p).

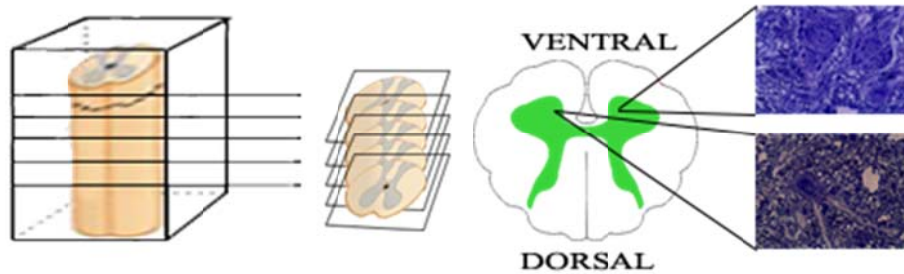


Figure 23. T11 segment of Spinal cord sectioning and motor neuron counting protocol. 6-days diabetic and T11segment of spinal cords were embedded in epon. The region was serially sectioned into 1- μ m thin sections spaced 100 μ m apart. Five sections from region were stained with toluidine blue to visualize motor neurons within the anterior horns of the spinal cord. Left and right anterior horns were photographed in four 100 \times fields using light microscopy. Total motor neuron population and area were measured from each field using computer-assisted imaging software.

$$N = \bar{Q} \times \Sigma_p \times k \times \frac{(a/p)}{a_{(frame)}}$$

N = Total Number, \bar{Q} = averaged objects, Σ_p = Total number of volumetric dots

K = section thickness, **a** _(frame) = frame area.

Statistical analysis of these obtained data (total mean neuron number and motor neuron cells area) was performed. Descriptive statistics for the motor neuron area, and the total number of motor neuron, relative to all obtained data related to values; median is expressed as mean, standard deviation, minimum and maximum

value. Kruskal-wallis test was used to compare the groups in terms of these characteristics. The statistical significance level in the calculations was taken as 5% and the calculations were a computer program for statistical analysis, the version statistical package for the social sciences (Version: 13) was done in statistical package program. P value was larger than 0.05 were considered statistically not significant (Table 4).

10% Neutral Buffered Formalin (NTF)

40% formalin	100 ml
Distill water.....	900 ml
Sodium phosphate, monobasic, monohydrate	4 gr
Sodium phosphate, dibasic, anhydrous	6.5 gr

Epon Preparation:

Analytical.....	15 ml
DDSA	15 ml
Dibutyl phthalate	0,75 ml
Dimethyl Benzyl Amine.....	0,75 ml

3.3. Histological Staining Process

1. Excised the sample T11 Segment (2 mm) from Spinal Cord of rat after Thoracic Vertebrectomy.
2. Detached tissues were suspended for 2.5 hours in 2.5% Glutaraldehyde (+4 °C)
3. 1% Osmium Tetroxide was left for 2 hours (+ 4 °C).
4. It was allowed to stand for 10 minutes on the 5th alcohol series. (60%, 70%, 80%, 90% and 96% (2))
5. Propylene oxide was left to stand at room temperature twice for 10 minutes.
6. Propylene Oxide / Epon (1: 1 ratio) mixture was allowed to stand at room temperature for 1 hour.
7. The mixture was allowed to stand in a mixture of Propylene Oxide: Epon (1: 2 ratio) for 1 night.
8. The extracted tissue samples were then encapsulated.
9. Capsules were placed in 60 °C Oven instrument for 12 hours.
10. Tissue blocks were trimmed with a trim tool to open the cross-section.
11. Glass blades were used for sectioning.
12. Ultra-Microtome was then used to take very thin sections.
13. Semi-thin sections with a thickness of 1 µm were taken and placed on the slide.
14. Once the receiving sections were stuck with the heating machine, Boraxed Toluidine blue was added.
15. It was left on the Reheating Machine so that it could dry completely and penetrate the tissues.
16. Then the stream was waited until the excess of the paint had gone and the textures became clear.
17. Prepared Preparations were examined by Light-Microscope.

Toluidine Blue with Borax:

Toluidine Blue1 gr
Distill water.....100 ml
Sodium borate (borax)2 gr

3.4. Chemical Substances Used

1. Toluidine Blue
2. Pure Epon
3. Ethanol
4. Ketalar anesthesia (Pfizer)
5. Glutaraldehyde
6. Formaldehyde
7. Sodium borate (borax)
8. Dimethyl Benzyl Amine
9. Dibutyl phthalate
10. DDSA (Dodecanyl Substituted Anhydride)
11. Araldite
12. Propylene oxide
13. Osmium Tetroxide (OsO₄)

3.5. Devices

1. Oven, Wiseven Made in Korea.
2. Tracing, EM Trima-1170 Wien Made in Austria.
3. Ultramicrotome, Leica Ultracut UCTA-1170 Wien Made in Austria.
4. Computer, Sony Trinitron Multi Scan G520.
5. The camera, Sony DSC-S58 Made in Japan.
6. Painting vessels made in Turkey.
7. Glass Knives
8. Light Microscope, Zeiss axioskop 40 Göttingen / Germany.
9. Photo attachment, Zeiss AxioCam HRc (CAM) Carl Zeiss vision GmbH Germany.
10. Heated Stirrer, EM Wisestir MSH 20A.
11. Glass Knife maker Leica, EM KMR2A-1170 (Wien Made in Austria).
12. The instrument, IME-DC (Made in China).

13. Refrigerators, Beko 8460T (Made in Turkey).
14. Leica Microsystems GmbH.
15. Sensitive Balance, Precisa XB 4200C Switzerland.
16. Disposable Polyethylene Eye Dropper



4. RESULTS

In rats, there were not observed abnormalities in behaviors or feeds daily or the drinking rate in the control categories and saline group categories. Opposed to them in the group rats suffered from excessive of water drinking and Polyuria, drowsiness and decreased interest in feeds.

4.1. Statistical Description

Statistically, the total volume and motor neuron counts were calculated for control, physiology saline, 45mg/kg, and 65mg/kg group by dissector-cavalier combinations that present in the science of stereological method. The Microsoft SPSS Version 13.0 program was used for statistical analysis and the Kruskal-Wallis test was used for comparisons between groups.

The weights of control and saline group categories changes there was not considerable in. Dissenting to these two groups there was a statistically considerable losing in weight of streptozotocin (STZ) groups rats (Table 1 and 2). We took blood from rats two times, on the 2nd day and one day before the sacrifice. The blood glucose rate was between normal range 75-125 mg/dl in the control and saline group categories (Table 3). But in the G45 and G65 categories after 3 days of injection by STZ the rate of glucose in the blood increased, more than 200 mg/dl and that mean these categories have diabetes (Table 3).

Stereological findings

Borax toluidine blue stain was added to T11 segment sections (Toth et al, 2008). By light microscope, slide sections of all experimental rats were examined. The structures of gray matter and motor neurons were normal. The total mean numbers and the total volume area of motor neuron in each category were compared to the control category. The results were no significant differences between groups (Table 4 and 5). Results more appeared in the images (Figure 24-32).

Table 1. Net weight and percentage lost until the end of the experiment (g).

Groups	Prior to the experiment(g)	Before sacrificed	Difference(g)	Percentage Change
Control	164.3	172.3	8	%4.8
Saline group	208	211	3	%1.4
45 mg	229.7	203.6	-26.1	-%11.3
65 mg	222	181.4	-40.1	-%18

Table 4. Descriptive statistics and comparison results by groups for the features motor neuron number.

n		Median	Mean	St. Dev.	Min.	Max.	P
Groups	Control	3751,8	3489,4	745,1	2145,0	4212,0	,232
	S	3463,2	3183,4	708,9	2174,4	3985,8	
	G45	2489,4	2882,3	639,8	2340,0	3940,2	
	G65	2181,6	2682,9	899,0	2095,2	4546,8	

Measurements are mean \pm SEM.

Table 2. Weight change in groups by (g) unit, during the experimental period.

Group	First day Pre-test weight	Last day Post-test weight
Control 1	158 g	160 g
Control 2	152 g	161 g
Control 3	182 g	192 g
Control 4	166 g	174 g
Control 5	168 g	174 g
Control 6	164 g	168 g
Control 7	160 g	178 g
Saline group 1	198 g	196 g
Saline group 2	218 g	217 g
Saline group 3	210 g	211 g
Saline group 4	228 g	227 g
Saline group 5	192 g	191 g
Saline group 6	214 g	222 g
Saline group 7	196 g	213 g
45 mg/kg 1	230 g	219 g
45 mg/kg 2	222 g	206 g
45 mg/kg 3	228 g	196 g
45 mg/kg 4	242 g	223 g
45 mg/kg 5	208 g	183 g
45 mg/kg 6	256 g	224 g
45 mg/kg 7	222 g	174 g
65 mg/kg 1	226 g	162 g
65 mg/kg 2	220 g	186 g
65 mg/kg 3	206 g	170 g
65 mg/kg 4	240 g	188 g
65 mg/kg 5	220 g	158 g
65 mg/kg 6	240 g	212 g
65 mg/kg 7	202 g	194 g

Table 3. Blood glucose levels change by (mg/dl) unit, in groups before and after the injection.

Group	Fasting blood glucose level before(mg/dl) injection to STZ	Fasting blood glucose level After(mg/dl) injection to STZ
Control 1	83 mg/dl	99 mg/dl
Control 2	86 mg/dl	70 mg/dl
Control 3	89 mg/dl	71 mg/dl
Control 4	75 mg/dl	80 mg/dl
Control 5	101 mg/dl	83 mg/dl
Control 6	82 mg/dl	77 mg/dl
Control 7	90 mg/dl	82 mg/dl
Saline group 1	79 mg/dl	84 mg/dl
Saline group 2	83 mg/dl	77 mg/dl
Saline group 3	91 mg/dl	81 mg/dl
Saline group 4	87 mg/dl	93 mg/dl
Saline group 5	82 mg/dl	90 mg/dl
Saline group 6	84 mg/dl	79 mg/dl
Saline group 7	76 mg/dl	80 mg/dl
45 mg/kg 1	87 mg/dl	315 mg/dl
45 mg/kg 2	79 mg/dl	366 mg/dl
45 mg/kg 3	94 mg/dl	379 mg/dl
45 mg/kg 4	78 mg/dl	301 mg/dl
45 mg/kg 5	96 mg/dl	405 mg/dl
45 mg/kg 6	80 mg/dl	600 mg/dl
45 mg/kg 7	87 mg/dl	474 mg/dl
65 mg/kg 1	88 mg/dl	386 mg/dl
65 mg/kg 2	76 mg/dl	410 mg/dl
65 mg/kg 3	82 mg/dl	365 mg/dl
65 mg/kg 4	83 mg/dl	454 mg/dl
65 mg/kg 5	90 mg/dl	402 mg/dl
65 mg/kg 6	89 mg/dl	382 mg/dl
65 mg/kg 7	97 mg/dl	450 mg/dl

Table 5. Total motor neuron number and area values.

The Motor Neuron Number		
Groups	Body of motor neuron(μm^3)	Localization area the body of motor neurons(μm^3)
Control 1	1.3	123250000
Control 2	1.3	120250000
Control 3	1.5	117000000
Control 4	1.3	116500000
Control 5	1	116500000
Control 6	1.1	81250000
Control 7	1.5	112250000
Saline group 1	1.3	111250000
Saline group 2	1.1	135750000
Saline group 3	1.2	129250000
Saline group 4	0.8	114250000
Saline group 5	1.2	120250000
Saline group 6	1.2	75500000
Saline group 7	1.3	127750000
45 mg/kg 1	1.1	115500000
45 mg/kg 2	1	97500000
45 mg/kg 3	0.9	115250000
45 mg/kg 4	0.85	173000000
45 mg/kg 5	0.9	113750000
45 mg/kg 6	0.8	123500000
45 mg/kg 7	1.1	149250000
65 mg/kg 1	0.7	125000000
65 mg/kg 2	1.8	105250000
65 mg/kg 3	1.2	94750000
65 mg/kg 4	1.2	75750000
65 mg/kg 5	0.8	110000000
65 mg/kg 6	1.1	114250000
65 mg/kg 7	0.9	97000000

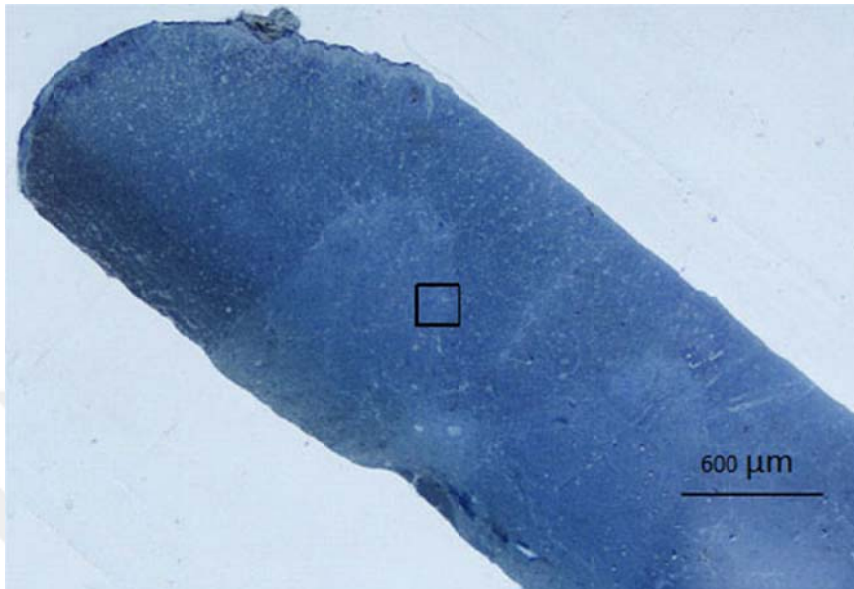


Figure 24. Control group Rat number 4 – cross section number 3, 4 x lens magnification (600μm). The square, showing the location on which we focused.

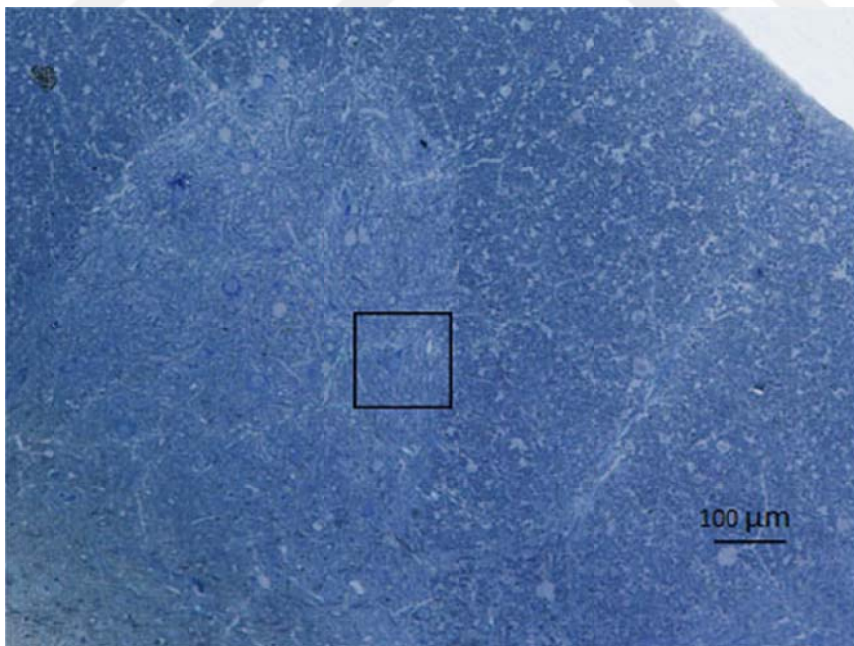


Figure 25. Control group Rat number 4 – cross section number 3, 10x lens magnification (100μm).

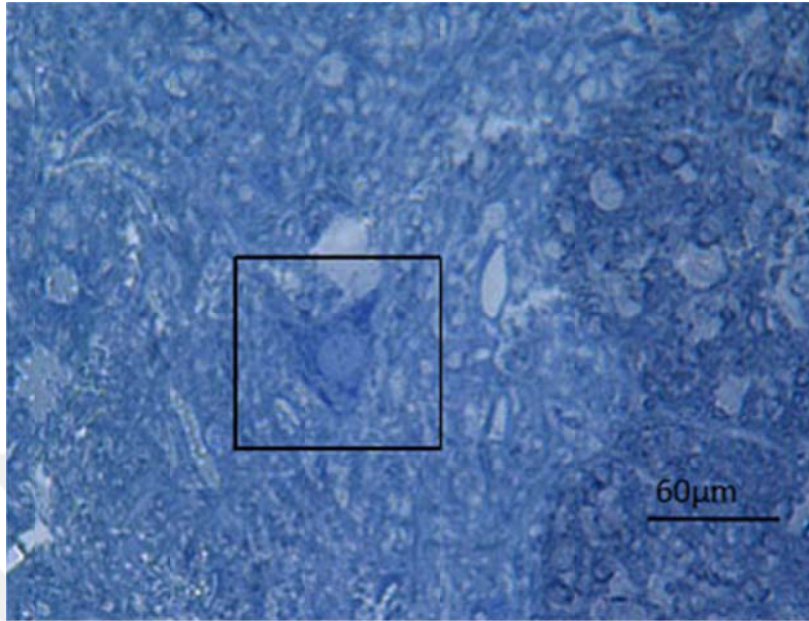


Figure 26. Control group Rat number 4 – cross section number 3, 40x lens magnification (60µm) motor neuron cell.

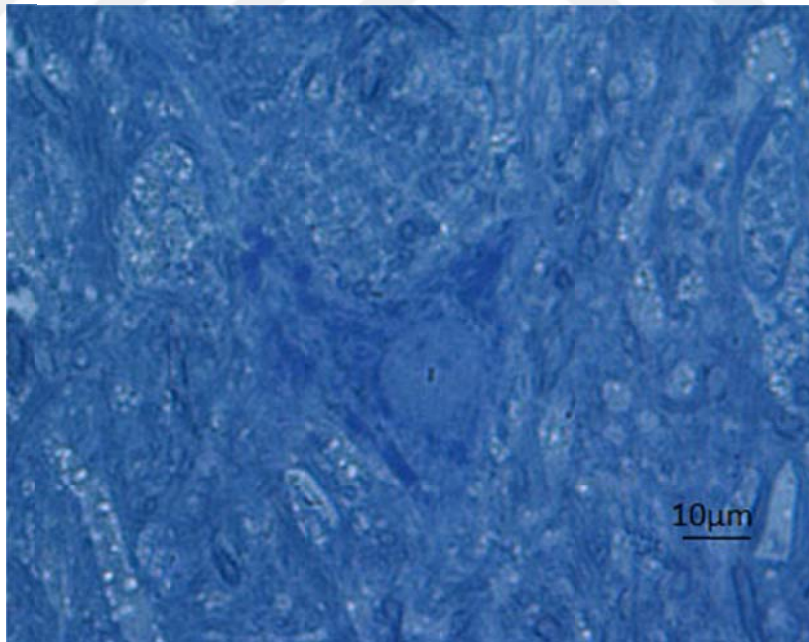


Figure 27. Control group Rat number 4 – section number 3, 100x lens magnification (10µm), motor neuron cell.

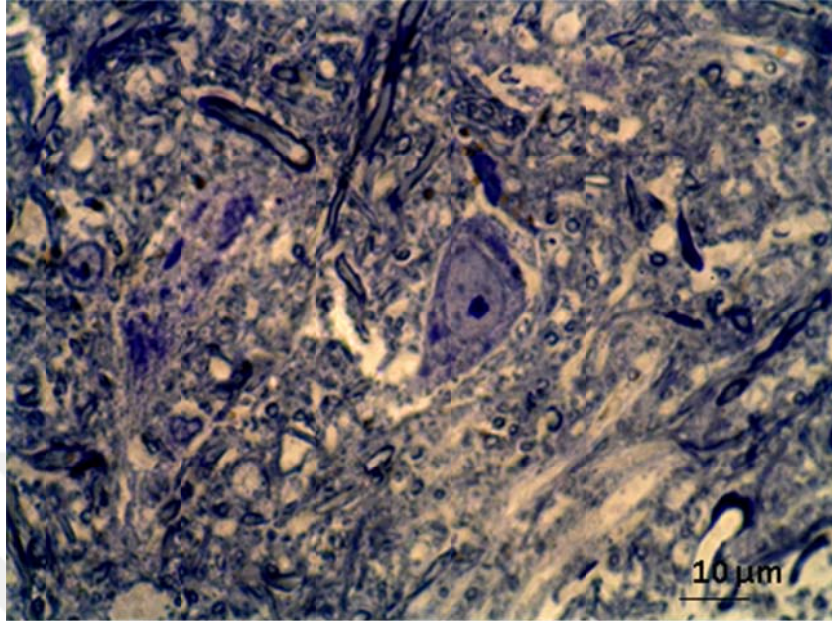


Figure 28. G45 group, Rat number 3 – cross section number 1, 100x lens magnification (10μm), motor neuron cell.

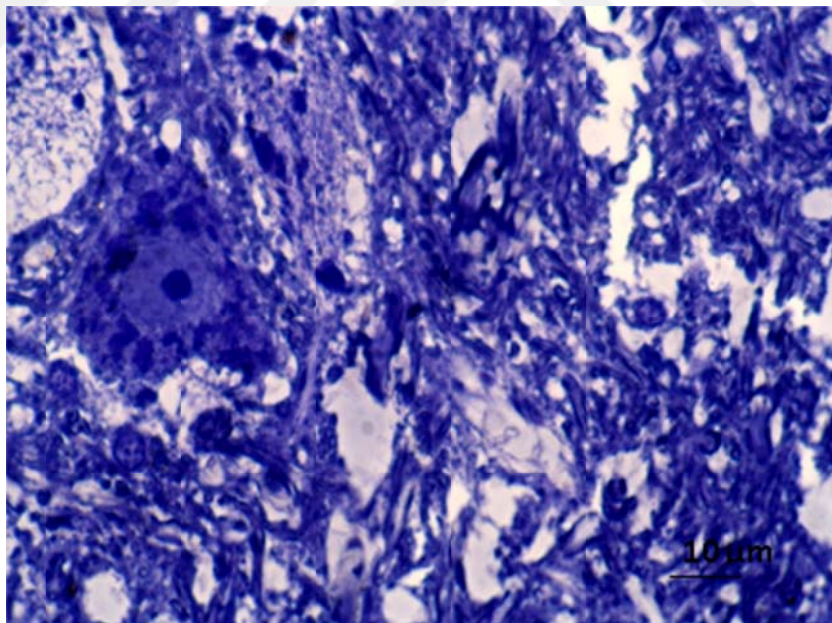


Figure 29. Saline group, Rat number 2 – cross section number 5, 100x lens magnification (10μm).

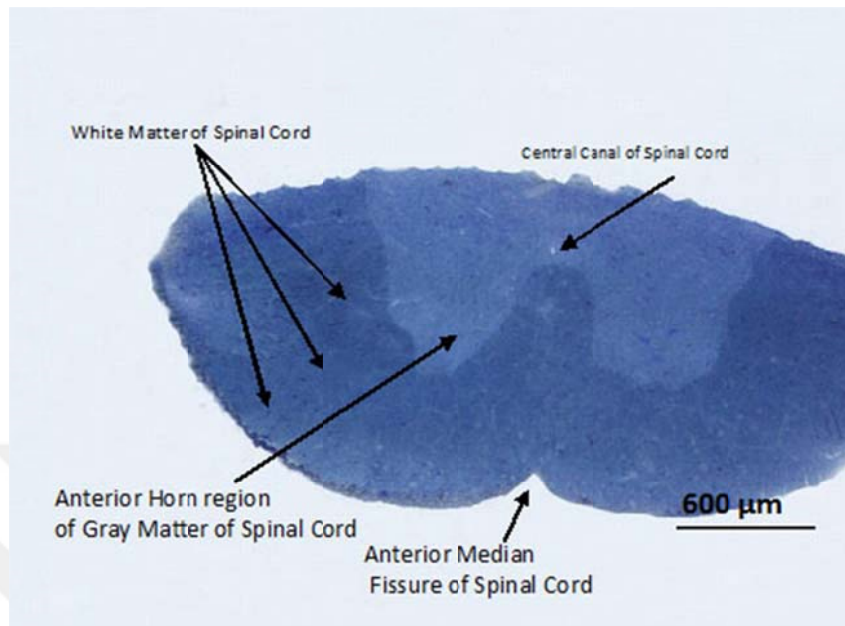


Figure 30. Control group Rat number 6 – cross section number 3, 4x lens magnification (600μm), T11 Segment of spinal cord.

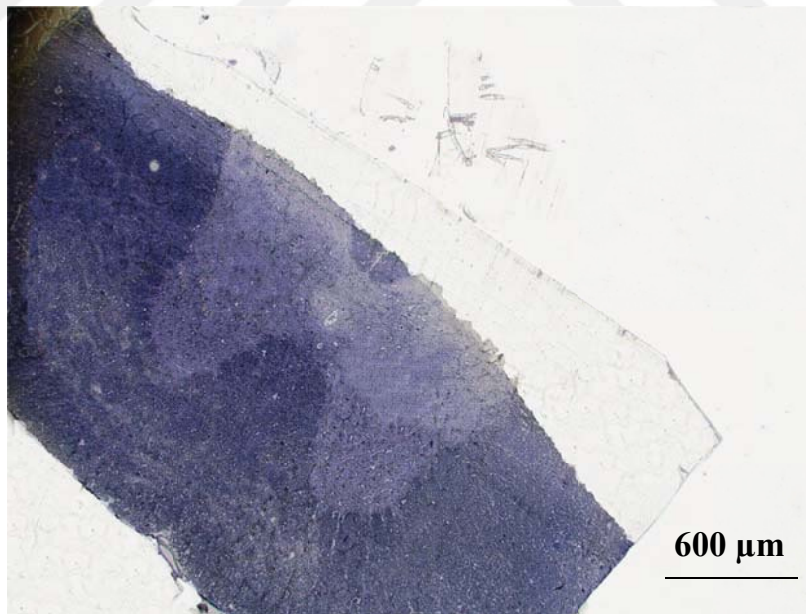


Figure 31. G65 group Rat number 6 – cross section number 2, 4x lens magnification (600μm), T11 Segment of spinal cord.



Figure 32. Saline group Rat number 1 – cross section number 1, 4x lens magnification (600 μ m), T11 Segment of spinal cord.

5. DISCUSSION AND CONCLUSION

Diabetes mellitus characterized by hyperglycemia increasing glucose level in the blood resulting from trouble in insulin excretion, insulin job, or both (American Diabetes Association, 2014). Diabetes causes many abnormalities in the human body organs or it has caused many disorders in different organs, including nervous system disease named as diabetic neuropathy (Boulton et al., 2005). One of the ten killer infections on the Earth for human genes is the Diabetes mellitus (WHO, 2014).

Insulin Synthesized by the β -cells of pancreatic islets is of major physiological importance in metabolic homeostasis. Two chains of polypeptide joined by disulphide bridges are produced ripe insulin, the gene encodes for a highly conserved single chain precursor, preproinsulin (Melloul et al., 2000).

Insulin produced by pancreas, it is the essential hormone that controls the take-up the basic unit sugar from the blood stream to the most smaller building unit inside organs are known as cells, particularly live (Iozzo et al., 2003), fat tissue (Abel et al., 2001) and muscle, aside from smooth muscle, in which insulin acts via the IGF-1 (Devol et al., 1990). So, incapability of insulin or the weakness of its receptors plays a central role focal part in all types of diabetes mellitus (American Diabetes Association, 2014). Diabetes defined by the higher level of glucose in the bloodstream for a long period. Diabetes mellitus causes much another disease as a side effect, such as Cardiomyopathy, Cardiovascular disease (Hamilton et al., 2007) and Renal Failure (Ritz et al., 1999).

Streptozotocin restrains insulin discharge and causes a condition of insulin-ward diabetes mellitus. Both impacts can be credited to its particular concoction properties, to be specific its alkylating power. Likewise with alloxan, its beta-cell specificity is for the most part, the consequence of particular cell take-up and aggregation (Lenzen, 2008).

Distinctive dosage infusions of streptozotocin in rats delivered pancreatic insulinitis, with development to practically whole β -cell devastation and diabetes mellitus. The planning and appearance of the provocative islet injuries recommend. Streptozotocin (STZ) is an expansive range antibiotic having antitumor, oncogenic, and

diabetogenic, properties. The last activity is intervened by pancreatic beta-cell devastation and is widely utilized as a strategy for the enlistment of diabetes in trial creatures and for clinical treatment of threatening β -cell tumours (Like and Rossini, 1976).

Type I diabetes (T1D) is associated with an "encephalopathy" clarified by a couple of components typical to the developing technique, degenerative and valuable bunches of the central tactile framework. In the present audit, they depict a show hyperactivity of the hypothalamic pituitary adrenal (HPA) hub in two unmistakable trial mouse models of T1D including the pharmacological one started by streptozotocin and the unconstrained diabetic mice (Beauquis et al., 2008).

To knowing whether diabetic has the impact on the motor neuron in the T11 fragments of the spinal cord or not at early diabetes? We infused the exploratory rats by various measurements of streptozotocin. Streptozotocin is one of the wide anti-toxins compounds that used to actuating diabetes in the experimental animal (Bolzán and Bianchi, 2002). After harm the β cells in pancreas the diabetic Mellitus type one delivering (Szkudelski, 2001) inside 2-4 days as it were (Akbarzadeh et al., 2007).

The outcomes of spinal rope damage differ contingent upon the size and seriousness of the harm. Spinal cord damage may cut off ordinary correspondence with the mind that can bring about a total or inadequate harm. A total harm brings about an aggregate absence of tactile and engine work underneath the level of damage. On account of a deficient harm, the capacity of the spinal cord to pass on messages to or from the mind is not totally lost. This sort of harm empowers a man to keep up some engine or tactile capacity beneath the damage, for T11 may be functional trouble happen in the muscles and glands, of the urinary system and uterus of women and some part of large and small intestinal and sense of those organs (Holroyd et al., 1995).

Sidenius and Jakobsen, (1980) in their studies, they used Male Wistar rats, 24-week of age weighing between 350 and 450 g, group of them injected with 40mg/kg of STZ, and after induced diabetes, from them separated 12 rats like a diabetic group and from the not inject 12 individual as the control group. After a four week, experimental period took a sample from anterior horn of the L5 segment and of the L5 dorsal root

ganglion. And by the stereological method measured the perikaryal substance volumes inside the sensory and motor neuron cells, and measured nucleoli nuclei by the same method. In their result reached to, is the perikaryal substance (Nissl substance) volume in those cells reduced but the sizes of nucleoli and nuclei were not changed, from there statically they reached to actual that no differences were observed of the variance of the diameter ratios between the two groups. And the number of this cells especially motor neuron not different or degeneration of nerve cells not observed (Sidenius and Jakobsen, 1980).

Noor Ramji and his colleagues at work, researched on the does diabetes mellitus target motor neurons, used, streptozotocin which dissolved in the citrate buffer by three differences concentration (45, 65, and 85mg/kg/day respectively) that inducing diabetic. For this purpose were used one-month-old mice and injected intraperitoneal, respectively, and test tail vein testing, during the experimental period, observed loss weight between diabetic groups reduced. Electrophysiology for motor neuron took every month in the same time multifibre motor conduction was registered. The motor entity number evaluated and single motor units potential were measured. The analysis of motor neurons morphometric performed to the cervical and lumbar segment of the spinal cord that took. Those tissue fixed in the glutaraldehyde (2.5%) for 1day in osmium tetroxide (2%) post-fixed in alcohols dehydrated and in the epon implanted, prepared to semi-thin cutting (1µm thickness). Electrophysiology of motor cells decreased but the statistical analysis and morphometry of motor neuron shown that the modification in the motor neuron cells number not happened (Ramji et al., 2007), in 2008 Ramji and Zochodne again made sure on that motor neurons are not main targets by diabetes mellitus (Zochodne et al., 2008).

Motor end plate innervation loss that is one of the faces of diabetic neuropathy, one of the problems that produce during diabetic, for that a group of researchers worked on this problem and used two ways to give insulin to understand the volume of damages happened by sugar disease, to prevent this damage and the way that is better. Tow group of mice in a long-term model daily delivered the insulin, one group insulin was transmission by intra-nasally and another group by subcutaneous insulin. In their work used Immunohistochemistry method to estimation the motor cells sample in lamina IX

were calculated at the cervical level (C5-7), thoracic (T6-8), or lumbar spinal cord (L4-6), with different regions having nonoverlapping neurons examined, hindlimb grip test, and western immunoblotting (the analytical technique used in molecular science). Into the end, the consequences of those two gatherings were compared to the control categories. By nonparametric testing using kruskal-wallis one-way analysis of variance testing was performed. The research team evaluated the morphometric analysis of spinal cord, peripheral nerve, muscle innervation, and specific molecular markers at and before the end point. They arrived at the point they said, despite the progressive distal axonal terminal loss, numbers and ability of motor body cells were protected (Francis et al., 2011).

In all articles before, the losing of weight and raised the glucose level from the normal range were two characteristics of the diabetic group that recognized. The loss of weight caused because of the cells was damaged. The raising of glucose it happened because of the glucose not entering the cells to burning it or the cells does not have the ability to taking the glucose (Sidenius and Jakobsen, 1980; Ramji et al., 2007; Francis et al., 2011).

To understand the ability of motor neuron remaining without significant effect during diabetes disease for a long time compared to other neurons cells there were two reasons. The first reason the motor neuron showing defiance to prevent the losing of his composition for a length period diabetes model of empirical animal but this defiance is weak in sensory neurons. The second reason the motor neuron that affected by diabetes, by illustrating the terminal retraction reverse the process at play in neuropathy and diabetic neurodegeneration. In the event that withdrawal and additionally withdrawal of terminals without straight to the point neuronal misfortune were illustrated, instead of hopeless drop out of perikarya, it would have critical ramifications for future endeavors at treatment (Ramji et al., 2007).

Our recommendation is to evaluate the number of synapses with transmission electron microscope and stereological method. As the stereological sub-method of the dissector-cavalieri combination was applied to estimation of the total mean number of motor neuron in our study. Due to influence of the cross-section thickness measurement

and the tissue shrinkage for following was eliminated (Pakkenberg and Gundersen, 1988).

In literature been reported the same resulted. The result is the numbers motor neuron statically not changed. In this time the diabetes was and remain one of the dangers diseases in the world (WHO, 2014) and all faces of this disease are not founded and information about his damages at the first step. We require more research to understanding diabetes to founding a good way to prevent his side effect for the disease (Sidenius and Jakobsen, 1980). May be it true, that diabetes in the primary stage does not affect motor neuron but diabetes by damage of distal axon and motor end plate does not stop and eventually causing major problems that may not be retrieved (Sidenius and Jakobsen, 1980; Gundersen et al., 1988; Ramji et al., 2007; Zochodne et al., 2008).

Conclusion: In our studies, we arrived at the result that the number and volume area of motor neuron not changed, when compared between the experimental diabetic group and non-diabetic group, control group with saline group, and between the low doses of STZ injected group and the higher dose of STZ injected group. These two results were measured by the stereological method. The analysis of static was founded by Microsoft SPSS (version 13.0), and we performed comparisons between groups by the Kruskal-Wallis test. It is very important, by molecular diagnosis, cytopathology with histopathology examine all part of the motor neuron (soma, axon hillock to the end plate of the axon and spinal root nerve), to determine the damage or change that is caused by diabetes.

SUMMARY

RAHIM Omer O, A stereological study on the motor neuron number in spinal cord segment T11 in different doses of streptozotocin administered rats. Yuzuncu Yil University, Institute of Health Science, Department of Medical Histology and Embryology, Master Thesis, Van-2017. Motor neuron cells in the spinal cord are responsible for transmitting the impulses from the brain to the peripheral of the body especially to muscles and glands. Streptozotocin (STZ) is extensively utilized to stimulate empirical diabetes in animals by destroying the β cells of the pancreas. The areas and composition of the nervous tissue in the body are different for this reason the effect of diabetes on the neurons and their parts vary. The motivation behind this project is to explore the impacts of STZ at different doses on the motor neuron in the T11 segment of the spinal cord by the stereological methods. The stereological method which we used in this study proved that the experimental diabetes mellitus do not affect the motor neuron number in the T11 segment of the spinal cord. Those twenty-eight rats used in this work were divided into four equal groups; control group, saline group, 45 mg/kg STZ injected group and 65 mg/kg STZ injected group. Median weight of rats was recorded as 200g on the first day. The level of blood sugar and weights of rats prior to the experiment and final day of work were recorded. The T11 section was prepared for microscopically investigation and the photo was taken. The total volume and motor neuron counts were calculated for each group using dissector-cavalier combinations of the stereological method. The SPSS version 13.0 program was used for statistical analysis. The comparisons between groups were performed by kruskal-wallis test. The result showed that there was no significant difference between groups ($P>0.05$). Total number of motor neuron was not differed among groups.

Key word: Spinal cord, T11 segment, Motor neuron number, Streptozotocin, Stereology

ÖZET

RAHİM Omer O, Farklı dozlarda streptozotocin uygulanan sıçanların medulla spinalis T11 segmentinde motonöron sayısı üzerine sterolojik bir çalışma.Yüzüncü Yıl Üniversitesi, Sağlık Bilimleri Enstitüsü, Tıbbi Histoloji ve Embriyoloji Anabilim Dalı, Yüksek lisans Tezi, Van-2017.

Medulla spinalis motor nöron hücreleri, beyinden vücudun periferine özellikle kas ve bezlere uyarı iletiminde sorumludur. Streptozotocin, pankreasın β hücrelerini yok ederek hayvanlardaki deneysel diyabeti uyarmak için yoğun olarak kullanılmaktadır. Vücuttaki sinir dokusunun alanları ve bileşimi farklıdır, bu yüzden diyabetin nöronlar ve nöron uzantıları üzerindeki etkisi değişiklik gösterir. Bu projenin amacı, farklı dozlarda STZ'nin omuriliğin T11 segmentindeki motor nöron üzerindeki etkilerinin stereolojik yöntemlerle araştırmaktır. Bu çalışmada kullandığımız stereolojik yöntem, deneysel diabetes mellitusun omuriliğin T11 segmentindeki motor nöron sayısını etkilemediği kanıtlandı. Bu çalışmada kullanılan yirmi sekiz sıçan dört eşit gruba ayrıldı. Kontrol grubu, Salin grubu, 45 mg/kg STZ enjekte edilen grup ve 65 mg/kg STZ enjekte edilen grup. İlk gün Sıçanların ortalama ağırlığı 200 gr olarak ölçüldü. Deney ve çalışmanın son gününden önce ratların vücut ağırlıkları ve kan şekeri düzeyleri kaydedildi. T11 segmenti mikroskopik inceleme için hazırlandı ve fotoğraf çekildi. Stereolojik yöntemin disektor-Cavalieri kombinasyonu kullanılarak her grup için toplam volüm ve motor nöron sayıları hesaplandı. İstatistiksel analiz için SPSS version 13.0 programı kullanılmış. Gruplar arasındaki karşılaştırmalar Kruskal-Wallis testi kullanılmış. Sonuçlar gruplar arasında anlamlı bir fark olmadığını gösterdi ($P>0.05$). Toplam motor nöron sayısı gruplar arasında farklılık göstermedi.

Anahtar Kelimeler: Spinal kord, T11 segmenti, Motor nöron sayısı, Streptozotosin, Stereoloji

REFERENCES

Abel ED, Peroni O, Kim JK, Kim Y, Boss O, Hadro E, Minnemann T, Shulman GI, Kahn BB (2001). Adipose-selective targeting of the GLUT4 gene impairs insulin action in muscle and liver. *Nature*, 409, 729–733.

Abercrombie M (1946). Nuclear population from micotome sections. *Anat Rec*, 94, 239–247.

Ahmed A (2002). History of diabetes mellitus. *Saudi Med J*, 23, 373–378.

Akbarzadeh A, Norouzian D, Mehrabi MR, Jamshidi S, Farhangi A, Verdi AA, Rad BL (2007). Induction of diabetes by streptozotocin in rats. *Indian Journal of Clinical Biochemistry*, 22, 60–64.

Alarcon-Aguilar FJ, Estrada MJ, Chilpa RR, Paredes BG, Weber CC, Roman-Ramos R (2000). Hypoglycemic activity of root water decoction, sesquiterpenoids, and one polysaccharide fraction from *Psacalium decompositum* in mice. *J Ethnopharmacol*, 69, 207–215.

Alberti KGMM, Zimmet PZ (1998). Definition , diagnosis and classification of diabetes mellitus and its complications part 1 : Diagnosis and classification of diabetes mellitus provisional report of a WHO consultation. *Diabet Med*, 15, 539–553.

Altunkaynak B (2012). A brief introduction to stereology and sampling strategies: basic concepts of stereology. *neuroQuantology*, 10, 31–43.

American Diabetes Association (2000). Type 2 diabetes in children and adolescents. *Pediatrics*, 105, 671–680.

American Diabetes Association (2014). Standards of medical care in diabetes. *Diabetes Care*, 37, S14–S80.

Andersen BB, Pakkenberg B (2003). Stereological quantitation in cerebella from people with schizophrenia. *Br J Psychiatry*, 182, 354–361.

Ayrancı E, Altunkaynak BZ, Aktaş A, Ragbetli MÇ, Kaplan S (2013). Prenatal exposure of diclofenac sodium affects morphology but not axon number of the median nerve of rats. *Folia Neuropathol*, 51, 76–86.

Bailes BK, Bakewell S (2002). Diabetes mellitus and its chronic complications. *AORN J*, 76, 266–282.

Baldock R, Morriss-kay G (2016). Spinal cord and peripheral nervous system. Kaufman's Atlas of Mouse Development Supplement with Coronal Sections, 1st Ed, p. 177–191, Elsevier; London.

Bardsley JK (2004). Overview of diabetes. *Crit Care Nurs Q*, 2, 106–112.

Barson AJ, Sands J (1977). Regional and segmental characteristics of the human adult spinal cord. *J Anat*, 12, 797–803.

Beauquis J, Homo-Delarche F, Revsin Y, Nicola AFD, FS (2008). Brain alterations in autoimmune and pharmacological models of diabetes mellitus: Focus on hypothalamic-pituitary-adrenocortical axis disturbances. *Neuroimmunomodulation*, 15, 61–67.

Benitez SU, Carneiro EM, De Oliveira ALR (2015). Synaptic input changes to spinal cord motoneurons correlate with motor control impairments in a type 1 diabetes mellitus model. *Brain Behav*, 372, 1–9.

Bolzán AD, Bianchi MS (2002). Genotoxicity of streptozotocin. *Mutation Research*, 51, 121–134.

Bornstein J, Lawrence RD (1951). Plasma insulin in human diabetes mellitus. *Br Med J*, 2, 1541–1544.

Boulton AJM, Vinik AI, Arezzo JC, Bril V, Feldman EL, Freeman R, Ziegler D (2005). Diabetic neuropathies: A statement by the american diabetes association. *Diabetes Care*, 2, 956–962.

Brown AG (1981). Spinal cord organization. Organization in the Spinal Cord the Anatomy and Physiology of Identified Neurones, 1st Ed, p. 12, Springer; Berlin.

Canan S, Şahin B, Odacı E, Bünyami Ü, Aslan H, Ragbatlı MÇ, Kaplan S (2002). Toplam hacim, hacim yoğunluğu ve hacim oranlarının hesaplanmasında kullanılan bir stereolojik yöntem: cavalieri prensibi. *Türkiye Klinikleri Tıp Bilimleri Dergisi*, 22, 7–14.

Clemente CD (2011). The back, vertebral column, and spinal cord. *Anatomy A Regional Atlas of the Human Body*, 6th Ed, p. 369–408, Lippincott Williams & Wilkins; Philadelphia.

Courteix C (1993). Streptozocin-induced diabetic rats: behavioural evidence for a model of chronic pain. *Pain*, 53, 81–88.

Courten MD (2002). Evidence-based definition and classification. *The Evidence Base for Diabetes Care*, 1st Ed, p. 13–36, John Wiley & Sons Ltd; England.

Deeds MC, Anderson JM, Armstrong AS, Gastineau DA, Hiddinga HJ, Jahangir AN, Eberhardt, Kudva YC (2011). Single dose streptozotocin induced diabetes: considerations for study design in islet transplantation models. *Lab Anim*, 45, 131–140.

Devlin TM (1997). Carbohydrate metabolism II: special pathways. *Textbook of biochemistry with clinical correlations*, 4th Ed, p. 336–351, Wiley-Liss; New York.

Devol AL, Rotwein P, Sadow JL, Novakofski J, Bechtel PJ (1990). Activation of insulin-like growth factor gene expression during work-induced skeletal muscle growth. *Am J Physiol*, 259, E89–E95.

Dorph-Petersen (2001). Tissue shrinkage and unbiased stereological estimation of particle number and size. *J Microsc*, 204, 232–246.

Eastham, Essex (1969). Use of tissues embedded in epoxy resin for routine histological examination of renal biopsies. *J Clin Pathol*, 22, 99–106.

Francis GJ, Martinez JA, Liu WQ, Zochodne DW, Hanson LR, Frey WH, Toth C, (2011). Motor end plate innervation loss in diabetes and the role of insulin. *J Neuropathol Exp Neurol*, 70, 323–339.

Ganda OP, Rossini AA, Boston LA (1976). Studies on streptozotocin diabetes. *Diabetes*, 25, 595–603.

Gartner LP, (2015). Overview-Nervous System. BRS Cell Biology and Histology, 7th Ed, p. 143-162, Lippincott Williams & Wilkins; Philadelphia.

Gartner LP, James LH (2007). Nervous tissue. Color Text Book of Histology, 3rd Ed, p. 185-206, Elsevier; New York.

Gispén, WH, Biessels G (2000). Cognition and synaptic plasticity in diabetes mellitus. *Trends Neurosci*, 22, 542–549.

Graham ML, Janecek JL, Kittredge JA, Hering BJ, Schuurman HJ (2011). The streptozotocin-induced diabetic nude mouse model: differences between animals from different sources. *Comp Med*, 61, 356–360.

Gundersen H, Bagger P, Bendtsen TF, Evans SM, Korbo L, Marcussen, N, Pakkenberg B (1988). The new stereological tools: disector, fractionator, nucleator and point sampled intercepts and their use in pathological research and diagnosis. *APMIS*, 96, 857–81.

Gundersen HJG, Bendtsen TF, Korbo L, Marcussen N, Miziller A, Nielsen K, Nyengaard JR, Pakkenberg B, Sizirensen FB, Vesterby A, Wes MJ (1988). Some new, simple and efficient stereological methods and their use in pathological research and diagnosis. *APMIS*, 96, 379–394.

Gundersen HJG, Østerby R (1981). Optimizing sampling efficiency of stereological studies in biology: or “Do more less well!”. *J Microsc*, 121, 65–73.

Gundersen HJG, Jensen EB (1987). The efficiency of systematic of systematic smapling in stereology and its prediction. *J Microsc*, 147, 229–263.

Hales CN, Barker DJP (1992). Type 2 (non-insulin-dependent) diabetes mellitus: the thrifty phenotype hypothesis. *Diabetologia*, 3, 595–601.

Hamilton MT, Hamilton DG, Zderic TW (2007). Role of low energy expenditure and sitting in obesity, metabolic syndrome, type 2 diabetes, and cardiovascular disease. *Diabetes*, 56, 2655–2667.

Heimer L (1983). Development of the nervous system; the spinal cord. *The Human Brain and Spinal Cord*, p. 9-164, Springer; New York.

Himsworth HP (1939). The mechanism of diabetes mellitus. *The Lancet*, 243, 171–176.

Hockfield S, McKay RDG (1985). Identification of major cell classes in the developing mammalian nervous system. *J Neurosci*, 5, 3310–3328.

Hodsdon WS, Raible DW, Wood A, Hodsdon W, Henion PD, Weston JA (1992). Segregation and early dispersal of neural crest cells in the embryonic zebrafish. *Dev Dyn*, 195, 29–42.

Hoftiezer V, Carpenter AM (1973). Comparison of streptozotocin and alloxan-induced diabetes in the rat, including volumetric quantitation of the pancreatic islets. *Diabetologia*, 184, 178–184.

Holroyd A, French DJ, Goreczny AJ (1995). Spinal cord injury. *Hand book of Health and Rehabilitation Psychology*, p. 341–360, Springer; New York.

Horikawa Y, Oda N, Cox NJ, Li X, Orho-melander M, Hara M, Bell GI (2000). Genetic variation in the gene encoding calpain-10 is associated with type 2 diabetes mellitus. *Nat Genet*, 26, 163–175.

Hosokawa M, Dolci W, Thorens B (2001). Differential sensitivity of GLUT1 and GLUT2 expressing β -cells to streptozotocin. *Biochem Biophys Res Commun*, 289, 1114–1117.

Hosseinzadeh H, Nassiri-asl M (2013). Avicenna's (Ibn Sina) the canon of medicine and saffron (*crocus sativus*): a review. *Phytother Res*, 24 (7), 475–483.

Iozzo P, Geisler F, Oikonen V, Maki M, Takala T, Solin O, Nuutila P (2003). Insulin stimulates liver glucose uptake in humans: An F-18-FDG PET study. *J Nucl Med*, 44, 682–689.

Kahn SE, Hull RL, Utzschneider K (2006). Mechanisms linking obesity to insulin resistance and type 2 diabetes. *Nature*, 444, 840–846.

Kaplan S, Canan S, Şahin Bö Ünal B (1997). Stereolojik metotlar ve uygulamaları kursu notları, Ondokuz Mayıs Üniversitesi Tıp Fakültesi Histoloji-Embriyoloji Anabilim Dalı, Samsun.

Karunanayake EH, Hearse DJ, Mellows G (1975). The metabolic fate and elimination of streptozotocin. *Biochem Soc Trans*, 3, 410–414.

Kimmel CB, Warga RM, Kane DA (1994). Cell cycles and clonal strings during formation of the zebrafish central nervous system. *Development*, 276, 265–276.

Ko GTC, Chan JCN, Yeung VTF, Chow C, Li JKY, Lau MSW, Mackay IR, Rowley MJ, Zimmet P, Cockram CS (1998). Antibodies to glutamic acid decarboxylase in young chinese diabetic patients. *Ann Clin Biochem*, 35, 761–767.

Kua J, Chenb H, Hea K, Yana Q (2016). Preparation and properties of epoxy resin-coated micro-sized ferrosilicon powder. *Mat Res*, 19, 889–894.

Kuzuya T, Nakagawa S, Satoh J, Kanazawa Y, Iwamoto Y, Kobayashi M, Nanjo K, Sasaki A, Seino Y, Ito C, Shima K, Nonaka K, Kadowaki T (2002). Report of the committee on the classification and diagnostic criteria of diabetes mellitus the committee of the japan diabetes society on the diagnostic criteria of. *Diabetes Res Clin Pract*, 55, 65–85.

Lawley PD, Shah SA (1972). Methylation of ribonucleic acid by the carcinogens dimethyl sulphate, n-methyl-n-nitrosourea and n-methyl-n'-nitro-n-nitrosoguanidine. comparisons of chemical analyses at the nucleoside and base levels. *Biochem J*, 128, 117–132.

Lawson KA, Meneses JJ, Pedersen RA (1991). Clonal analysis of epiblast fate during germ layer formation in the mouse embryo. *Development*, 113, 891–911.

Leahy JK, Bumbalo LM, Chen C (1994). Diazoxide causes recovery of p-Cell Glucose responsiveness in 90% pancreatectomized diabetic rats. *Diabetes*, 43, 173–179.

Lenzen S (2008). The mechanisms of alloxan and streptozotocin-induced diabetes. *Diabetologia*, 51, 216–226.

Lewis KE, Eisen JS (2003). From cells to circuits : development of the zebrafish spinal cord. *Prog Neurobiol*, 69, 419–449.

Like AA, Rossini AA (1976). Streptozotocin-induced pancreatic insulinitis: new model of diabetes mellitus. *Science*, 193, 415–417.

Lima D, Coimbra A (1986). A golgi study of the neuronal population of the marginal zone (lamina I) of the rat spinal cord. *J Comp Neurol*, 244, 53–71.

Malgaonkar M, Shirolkar A, Murthy SN, Pawar S (2016). Ayurvedic plants with antidiabetic potential. *Medicinal Plants-Recent Advances in Research and Development*, p. 439–468, Springer; Singapore.

Mandarim-De-Lacerda CA (2003). Stereological tools in biomedical research. *An Acad Bras Ciênc*, 75, 469–486.

Martin BC, Warram JH, Krolewski AS, Soeldner JS, Kahn CR, Martinb BC, Bergman RN (1992). Role of development in of type 2 diabetes mellitus : results of glucose and insulin resistance 25-year follow-up study. *The Lancet*, 340, 925-929.

Mccotter RE (1916). Regarding the length and extent of the human medulla spinalis. *Anat Rec*, 10, 559–564.

Medvei VC, Cornelius V (1982). Hsiao Kho Lun on diabetes mellitus at the end of the 7th century AD, *A History of Endocrinology*, 1st Ed, p. 87, Mtp Press Limited; Uk-Boston.

Melloul D, Marshak S, Cerasi E (2000). Regulation of insulin gene transcription. *Diabetologia*, 45, 309–326.

Mizushima N, Yoshimori T, Levine B (2010). Primer methods in mammalian autophagy research. *Cell Press*, 140, 313–326.

Moonen G (2014). *Development and characterization of an acute impact-compression lumbar spinal cord injury model in the rat*. Master of Science Thesis, Institute of Medical Science, University of Toronto.

Moonen G, Satkunendrarajah K, Wilcox JT, Badner A, Mothe A, Foltz W, Tator CH (2016). A new acute impact-compression lumbar spinal cord injury model in the rodent. *J Neurotrauma*, 33, 278–289.

Moore KL, Dalley AF, Agur AMR (2014). Contents of vertebral canal. Moore - Clinically Oriented Anatomy, 7th Ed, p. 440-501; Lippincott Williams & Wilkins, Philadelphia.

Moore KL, Persaud TVN, Torchia MG (2016). Nervous system. Before We are Born, 9th Ed, p. 252–275, Elsevier; Philadelphia.

Nicholas DS, Roy O (1988). The fine anatomy of the human spinal meninges. *J Neurosurg*, 69, 276–282.

Oliveira S, Nessler RA, Castania JA, Salgado C (2013). Ultrastructural and morphometric alterations in the aortic depressor nerve of rats due to long term experimental diabetes : effects of insulin treatment. *Brain Res*, 1491, 197–203.

Peterson RG, Shaw WN, Neel M, Little LA, Eichberg J (1990). Zucker diabetic fatty rat as a model for non-insulin-dependent diabetes mellitus. *ILAR J*, 32, 16–19.

Poretsky L (2004). The main events in the history of diabetes mellitus. Principles of Diabetes Mellitus, p. 19–37, Springer; New York.

Ramji N, Zochodne DW, Toth C, Kennedy J (2007). Does diabetes mellitus target motor neurons? *Neurobiol Dis*, 26, 301–311.

Rastogi SC (2007). Nerve physiology. Essentials of animal physiology, 4th Ed, p. 311–333, New Age; New Delhi.

Reaven GM (1988). Banting lecture 1988 role of insulin resistance in human. *Diabetes*, 37, 1595–1607.

Rexed B (1952). The cytoarchitectonic organization of the spinal cord in the cat. *J Comp Neurol*, 96, 415–495.

Risch N (1987). Assessing the role of HLA-linked and unlinked determinants of disease. *Am J Hum Genet*, 40, 1–14.

Ritz E, Rychli IK, Locatelli F, Halimi S (1999). End-stage renal failure in type 2 diabetes: a medical catastrophe of worldwide dimensions. *Am J Kidney Dis*, 34, 795–808.

Said G (2007). Diabetic neuropathy: A review. *Nature Clinical Practice Neurology*, 3, 331–340.

Sato KL, Sanada LS, Ferreira RDS, deMarco M, Salgado J, Nessler RA, Fazan VPS (2014). Renal nerve ultrastructural alterations in short term and long term experimental diabetes. *BMC Neurosci*, 15, 2–11.

Schein, O'connell, Blom, Hubbard, Magrath, Bergevin, Devita (1974). Clinical antitumor activity and toxicity of streptozotocin. *Cancer*, 34, 993–1000.

Schoenwolf GC (1985). Shaping and bending of the avian neuroepithelium: morphometric analyses. *Dev Biol*, 109, 127–139.

Schoenwolf GC, Bleyl SB, Brauer RP, Francis-West PH (2015). Development of the central nervous system. Larsen's Human Embryology, 5th Ed, p. 197–234, Elsevier; Philadelphia.

Schoenwolf GC, Delongo J (1980). Ultrastructure of secondary neurulation in the chick embryo. *Am J Anat*, 158, 43–63.

Schoenwolf GC, Smith JL (1990). Mechanisms of neurulation : traditional viewpoint and recent advances. *Development*, 109, 243–270.

Sidenius P, Jakobsen J (1980). Reduced perikaryal volume of lower motor and primary sensory neurons in early experimental diabetes. *Diabetes*, 29, 182–187.

Sterio DC (1984). The unbiased estimation of number and sizes of arbitrary particles using the disector. *J Microsc*, 134, 127–136.

Szkudelski T (2001). The mechanism of alloxan and streptozotocin action in B cells of the rat pancreas. *Physiol Res*, 50, 537–546.

Toth C, Rong LL, Yang C, Martinez J, Song F, Ramji N, Brussee V, Liu W, Durand J, Nguyen MD, Schmidt AM, Zochodne DW (2008). Receptor for advanced glycation, products (RAGEs) and experimental diabetic neuropathy. *Diabetes*, 57, 1002–1017.

Ünal B, Canan S, Aslan H, Şahin B, Çataloluk O, Kaplan S (2002). Doku örneklerindeki objelerin sayılarının hesaplanmasında tarafsız stereolojik metodlar: fiziksel disektör. *T Klin J Med Sc*, 22, 15–24.

Vasudevan DM, Sreekumari S, Vaidyanathan K (2013). Metabolic pathways of other carbohydrates. *Textbook of BIOCHEMISTRY for Medical Students*, 7th Ed, p. 137–146, Jaypee Brothers Medical Publishers; New Delhi.

Watson C, Paxinos G, Kayalioglu G (2009). Development of the spinal cord. *The Spinal Cord*, 1st Ed, 8–14, Elsevier, London.

Watson C, Paxinos G, Kayalioglu G (2009). The organization of the spinal cord. *The Spinal Cord*, 1st Ed, p. 1–7, Elsevier; London.

Weibel ER (1969). Stereological principles for morphometry in electron microscopic cytology. *Int Rev Cytol*, 26, 235–302.

West MJ, Slomianka L, Gundersen HJG (1991). Unbiased stereological estimation of the total number of neurons in the subdivisions of the rat hippocampus using the optical fractionator. *Anat Rec*, 497, 482–497.

WHO (2014). Media center the top 10 causes of death. www.who.int/mediacentre/factsheets/fs310/en.

Xu JY, Chan V, Zhang WY, Wat NMS, Lam KSL (2002). Mutations in the hepatocyte nuclear factor-1 α gene in chinese MODY families: prevalence and functional analysis. *Diabetologia*, 45, 744–746.

Yasui K, Hashizume Y, Yoshida M, Kameyama T, Sobue G (1999). Age-related morphologic changes of the central canal of the human spinal cord occluded type. *Acta Neuropathol*, 97, 253–259.


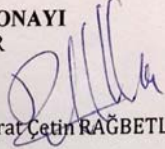
Ziegler AG, Jackson RA, Soeldner S, Eisenbarth GS (1990). Predicting type I diabetes. *Diabetes Care*, 13, 762–775.

CURRICULUM VITAE

Omed Omer RAHIM was born at 7/4/1978 in Sulaymaniyah city in the north of Iraq. In this city, he finished basic and high schools. In the University of Sulaimani started his first step, in academic higher education when he accepted as one of a student in the biological Department in Science College during the years (2002-2008). He got bachelor's degree in 2008. In 2009 in Sulaimani University accepted as the assistance Biology in the Biology Department till now his working there. During these 6 years, for one year he worked as a head of association green in Sulaymaniyah city in 2010 and for one year he worked as a main member of the Biological Syndicate in Sulaymaniyah in 2012. In 2014 he came to the Van city in the republic of Turkey, to starting the postgraduate admission process at the Yüzüncü Yıl University-Institute of Health Science, Faculty of Medicine-Histology and Embryology Department during the years (2014-2017). He was married at 2011 and has two children.





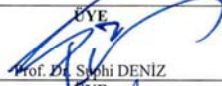
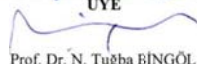
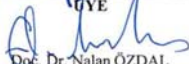

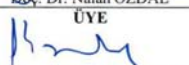

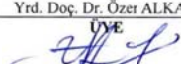
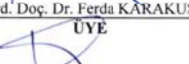
ATTACHMENTS
1. Plagiarism Result

YÜZÜNCÜ YIL ÜNİVERSİTESİ SAĞLIK BİLİMLERİ ENSTİTÜSÜ LİSANSÜSTÜ TEZ ORJİNALLİK RAPORU	
Tarih: 21/04/2017	
<p>Tez Başlığı / Konusu: Farklı dozlarda streptozotosinin uygulanan sıçanların medulla spinalis T11 segmentinde motonöron sayısı üzerine sterolojik bir çalışma.</p> <p>Yukarıda başlığı/konusu belirlenen tez çalışmamın Kapak sayfası, Giriş, Ana bölümler ve Sonuç bölümlerinden oluşan toplam 55 sayfalık kısmına ilişkin, 21 /04 /2017 tarihinde şahsım/tez danışmanım tarafından Turnitin intihal tespit programından aşağıda belirtilen filtreleme uygulanarak alınmış olan orijinallik raporuna göre, tezimin benzerlik oranı % 12 (on iki) dir.</p> <p>Uygulanan filtreler aşağıda verilmiştir:</p> <ul style="list-style-type: none">- Kabul ve onay sayfası hariç,- Teşekkür hariç,- İçindekiler hariç,- Simge ve kısaltmalar hariç,- Gereç ve yöntemler hariç,- Kaynakça hariç,- Alıntılar hariç,- Tezden çıkan yayınlar hariç,- 7 kelimedenden daha az örtüşme içeren metin kısımları hariç (Limit match size to 7 words) <p>Yüzüncü Yıl Üniversitesi Lisansüstü Tez Orijinallik Raporu Alınması ve Kullanılmasına İlişkin Yönergeyi inceledim ve bu yönergede belirtilen azami benzerlik oranlarına göre tez çalışmamın herhangi bir intihal içermediğini; aksinin tespit edileceği muhtemel durumda doğabilecek her türlü hukuki sorumluluğu kabul ettiğimi ve yukarıda vermiş olduğum bilgilerin doğru olduğunu beyan ederim.</p> <p>Gereğini bilgilerinize arz ederim.</p> <p style="text-align: center;"> Omed Omer RAHIM 21/4/2017 Tarih ve İmza</p>	
<p>Adı Soyadı: Omed Omer RAHIM Öğrenci No: 149302034 Anabilim Dalı: Tıp Fakültesi. Tıbbi Histoloji ve Embriyoloji Anabilim Dalı Programı: Tıbbi Histoloji ve Embriyoloji (Tıp) Statüsü: Y.Lisans <input checked="" type="checkbox"/> Doktora <input type="checkbox"/></p>	
<p>DANIŞMAN ONAYI UYGUNDUR</p> <p style="text-align: center;"> Prof. Dr. Murat Çetin RAĞBETLİ (Unvan, Ad Soyad, İmza)</p>	<p>ENSTİTÜ ONAYI UYGUNDUR</p> <p style="text-align: center;">(Unvan, Ad Soyad, İmza)</p>



T.C.
YÜZÜNCÜ YIL ÜNİVERSİTESİ
HAYVAN DENEYLERİ YEREL ETİK KURULU
ARAŞTIRMA KESİN SONUÇ ONAY BELGESİ

YUZUNCUYILUNIVERSITY (TURKEY)
ANIMAL RESEARCHES LOCAL ETHIC COMMITTEE
RESEARCH FINAL REPORT APPROVAL CERTIFICATE

Araştırmanın Adı	Farklı Dozlarda streptozotocin Uygulanan Sıçanların medulla spinalis T11 Segmentinde Motonöron sayısı Üzerine Sterolojik Bir Çalışma	
Title of the Research	A stereological study on the motor neuron number in spinal cord segment T11 in different doses of streptozotocin administered rats.	
Araştırmacı(lar) Investigator(s)	Yürütücü / Chief investigator : Prof. Dr. Murat Çetin RAĞBETLİ	
	Yardımcı Araştırmacı(lar) / Co-investigator(s): Omed Omer RAHİM	
Araştırmanın Başlama Tarihi / Research Starting Date:	13.12.2016	
Araştırmanın Bitiş Tarihi / Research Completion Date:	20.04.2017	
Proje Süresi / Total Time of Project:	6 ay/month	
Proje No / Project Number:	TYL-2016-5507	
Araştırmayı Destekleyen Kuruluş (varsa) / Funding institution(s) (if available):	YYU BAPB	
Destek Şekli ve Miktarı / Type and amount of funding:	YLTEZ / 4894,60	
Karar:	Yukarıda bilgileri verilen araştırma projesinin kesin sonuç raporu Yüzüncü Yıl Üniversitesi Hayvan Deneyleri Yerel Etik Kurulu'nun 25/05/2017 tarih ve 2017/05 sayılı kararı ile kabul edilmiştir.	
Decision:	Final report of the research project detailed above was approved by Yuzuncu Yil University Animal Researches Local Ethic Committee in the session held on 25/05/2017 (decision number 2017/05).	
	BASKAN/CHAIR	
	 Prof. Dr. Semiha DEDE	
 Prof. Dr. Fazıl ŞEN	ÜYE	 Prof. Dr. Sıddık KESKİN
ÜYE	ÜYE	ÜYE
 Prof. Dr. N. Tuğba BİNGÖL	Doç. Dr. Atilla DÜRMÜŞ	 Doç. Dr. Nalan ÖZDAL
ÜYE	ÜYE	ÜYE
 Yrd. Doç. Dr. Yıldırım BAŞBUĞAN	Yrd. Doç. Dr. Özer ALKAN	 Yrd. Doç. Dr. Ferda KARAKUŞ
ÜYE	ÜYE	ÜYE
 Yrd. Doç. Dr. Canser Yılmaz DEMİR	 Yrd. Doç. Dr. Orhan ALLAHVERDİYEV	 Zir. Müh. Kenan YILDIRIMOĞLU
ÜYE		
Vet. Hek. İsmail Hakkı BEHÇET		